American Mineralogist, Volume 66, pages 678–701, 1981

The structural role of aluminum in silicate melts—a Raman spectroscopic study at 1 atmosphere

BJØRN O. MYSEN, DAVID VIRGO AND IKUO KUSHIRO[1]

Geophysical Laboratory
Carnegie Institution of Washington
Washington, D. C. 20008

Abstract

The structural role of Al^{3+} in quenched silicate melts at 1 atm pressure as a function of composition has been explored with Raman spectroscopy. The compositions studied have sufficient or excess alkali or alkaline earth contents to balance the charge of Al^{3+} in tetrahedral coordination.

Aluminum was added as $CaAl_2O_4$, $NaAlO_2$ and Al_2O_3 to melts of $Na_2Si_2O_5$ and $CaSi_2O_5$ composition. Published spectroscopic data on quenched melts of these compositions indicate that their anionic structures consist of mixtures of units that have, on the average, NBO/Si = 2 (chain), 1 (sheet) and 0 (three-dimensional network) forming in bulk NBO/Si = 1 (NBO/Si; nonbridging oxygens per silicon). Whenever there is sufficient Na^+ in the melt to balance the charge of tetrahedral Al^{3+}, sodium is the charge-balancing cation whether or not Ca^{2+} is also present. With up to about 10 mole % Al_2O_3 (about 6 wt.%) all Al^{3+} enters the three-dimensional network structural unit. In the compositional range between 10 and 20 mole % Al_2O_3, aluminum occurs in both the three-dimensional network and the sheet structural units with a preference for three-dimensional network > sheet > chain structure.

In systems with only Ca^{2+} present, only two compositional regions may be defined. With up to 10 mole % Al_2O_3, Al^{3+} enters both three-dimensional network structures and sheet structures. With more aluminum, Al^{3+} enters all structural units with the same preference as in the sodic system.

On the basis of the present data and other published structural data on Ti^{4+}, P^{5+} and Fe^{3+} in quenched silicate melts, the anionic constitution of common igneous melts has been calculated. Almost all natural magmas have a ratio of nonbridging oxygen per tetrahedral cation (NBO/T) less than 1. Basalts have NBO/T between 0.9 and 0.6, andesitic melts have about 0.3 and granitic melts, between 0.2 and 0.05. The anionic structure of these melts can be described as mixtures of unit with NBO/T = 2, 1 and 0. In all melts, the three-dimensional network unit is the most aluminous. In general, acidic melts have higher Si/(Si+Al) of the structural units than basic melts. The value of this ratio in melts of igneous rocks is positively correlated with geochemical indicators such as Mg/(Mg+Fe^{2+}). The Si/(Si+Al) also is positively correlated with the activation energy of viscous flow of natural magma at 1 atm pressure.

Introduction

Knowledge of the structural role of Al^{3+} in igneous melts is important for several reasons. As a network former (Al^{3+} in tetrahedral coordination), the degree of polymerization of a melt (defined as the value of the ratio of nonbridging oxygens per tetrahedral cation; NBO/T) is linearly related to the amount of aluminum present in the melt. It has been suggested, however, that when pressure is applied to aluminous silicate melts, some or all of the Al^{3+} may no longer be in tetrahedral coordination (*e.g.*, Waff, 1975; Kushiro, 1976, 1978; Mysen, 1976; Mysen and Virgo, 1978). Furthermore, the possibility exists that Al^{3+} may not be in tetrahedral coordination if local charge-balance (with M^+ and M^{2+} metal cations) is not attained (Bottinga and Weill, 1972; Mysen *et al.*,

[1] Present address: Geological Institute, Faculty of Science, University of Tokyo, Hongo, Tokyo 113, Japan.

0003–004X/81/0708–0678$02.00

1980d; Wood and Hess, 1980). The latter suggestion implies that if the proportion of metal cations (alkalies and alkaline earths) in a magma is altered so that the magma becomes peraluminous, an amount of Al^{3+} equivalent to that in excess over the metal cation content will become a network modifier. Such a development would result in depolymerization of the melt, thus lowering its viscosity (Lacey, 1968), and would diminish the stability of highly polymerized liquidus minerals (Kushiro, 1975).

If Al^{3+} requires metal cations in its immediate vicinity in order to remain in tetrahedral coordination, the type of metal cation (*e.g.*, Ca^{2+} *vs.* Na^{+}) may affect the strength of bridging Al–O bonds. The bond energy associated with these bridges will control the stability of the aluminate complex. Physical properties of the melts such as density and viscosity may consequently be affected. It is known, for example, that the viscosity of $NaAlSiO_4$ melt is several times greater than that of $CaAl_2Si_2O_8$ melt (equal Si/Al) at the same temperature and pressure (Riebling, 1966; Cukiermann and Uhlmann, 1973), and the latter hypothesis may therefore be valid.

Virgo *et al.* (1980) and Mysen *et al.* (1980d) have proposed that binary metal oxide–silica joins as well as more complex silicate melts consist of three distinct types of structural units. They found that in the compositional interval between NBO/T = 4 and about 2.1, units with an average of 4, 3 and 2 NBO/T coexist. With bulk NBO/T between about 2.1 and 1.0 the structural units have NBO/T of 4, 2 and 1, whereas for melts that are more polymerized than that of bulk NBO/T = 1.0, the coexisting structural units have average NBO/T = 2, 1 and 0. Aluminum in tetrahedral coordination may be distributed between all these structural units in a random fashion, or there may be a distinct preference for one or more of the units. Preliminary data by Virgo *et al.* (1979) indicate that if the metal cation is Na^{+}, the aluminate complex may show a preference for three-dimensional network structures. It is not known, however, how other cations may affect the distribution of Al^{3+} between the polymeric units.

It is evident that variations of the structural role of Al^{3+} even in tetrahedral coordination will affect both chemical and physical properties of silicate melts. For example, the activity of a metal cation such as Ca^{2+} may depend on whether it charge-balances aluminum or it simply forms nonbridging oxygens in the melt. The relative stabilities of different aluminate complexes must consequently be known for a better understanding of liquidus phase relations as well as crystal–liquid trace element partitioning involving such elements.

With the above considerations in mind, a Raman spectroscopic study has been undertaken to determine some of the aspects of the structural role of aluminum in quenched silicate melts.

Starting compositions

Starting compositions (Table 1) were chosen with the following considerations in mind. First, what is the structural role of Al^{3+} in three-dimensional network structures when Na^{+} or Ca^{2+} or both charge-balance Al^{3+}? This subject has been discussed to a certain extent by Mysen *et al.* (1980d) and Virgo *et al.* (1979), and only a brief summary will be provided here. Second, what is the structural role of Al^{3+} when insufficient Na^{+} or Ca^{2+} is present for charge-balance? This subject will be discussed with compositions between $NaAlSi_7O_{16}$ and SiO_2 (90 wt.%)–Al_2O_3 (10 wt.%). The low Al_2O_3 content was chosen so that lack of spectral resolution due to Si(Al) coupling would be avoided (see Brawer and White, 1977; Virgo *et al.*, 1979; for discussion). A glass of $CaAl_2O_4$ composition was also studied in order to determine the characteristic Raman frequencies of Al^{3+} in tetrahedral coordination. Third, quenched melts with nonbridging oxygens on the joins Na_2O–SiO_2 and CaO–SiO_2 were studied. The anionic structure of binary and more complex quenched melts on these and other joins was determined by Mysen *et al.* (1980d). Their structural model may be summarized with these equations:

For NBO/T = 4.0–2.1:

$$Si_2O_7^{6-} = SiO_4^{4-} + SiO_3^{2-}, \quad (1)$$

for NBO/T = 2.1–1.0:

$$3SiO_3^{2-} = SiO_4^{4-} + Si_2O_5^{2-}, \quad (2)$$

and for NBO/T = 1.0–0.05:

$$Si_2O_5^{2-} = SiO_3^{2-} + SiO_2. \quad (3)$$

Mysen *et al.* (1980d) concluded that the ranges of NBO/Si within which each of these equations describes the equilibria are relatively insensitive to the type of metal cation(s) present. Aluminum was added to these quenched melts as $NaAlO_2$, $Ca_{0.5}AlO_2$ and Al_2O_3. In the first two cases, different charge-balancing cations were used to assess the effect of metal cations on the distribution of Al between the structural units in quenched melts that, in the absence of Al^{3+}, have bulk NBO/Si = 1 (NS2 and CS2

Table 1. Compositions of starting materials

	NS2	NS2 NA2.5	NS2 NA5	NS2 NA7.5	NS2 NA10	NS2 NA15	NS2 NA20	-	NS2 NA30	NS2 NA40
SiO_2	65.95	64.45	62.92	61.35	59.74	56.41	52.93	-	45.43	41.22
Na_2O	34.05	34.13	34.22	34.43	34.40	34.60	34.79	-	35.22	35.44
Al_2O_3	-	1.42	2.86	4.22	5.86	8.99	12.28	-	19.35	23.33
NBO/*T*	1.000	0.975	0.950	0.931	0.897	0.843	0.785	-	0.666	0.600
	-	NS2 CA2.5	NS2 CA5	-	NS2 CA10	NS2 CA15	NS2 CA20	NS2 CA25	NS2 CA30	NS2 CA40
SiO_2	-	64.52	63.07	-	60.06	57.19	54.21	51.15	47.34	41.79
CaO	-	0.77	1.55	-	3.12	4.17	6.32	7.96	10.01	13.00
Na_2O	-	33.31	32.57	-	31.06	29.54	27.99	26.41	24.44	21.58
Al_2O_3	-	1.40	2.81	-	5.76	8.56	11.48	14.48	18.21	23.63
NBO/*T*	-	0.976	0.951	-	0.899	0.834	0.801	0.750	0.688	0.760
	CS2	CS2 CA2.5	-	CS2 CA7.5	-	CS2 CA15	-	-	CS2 CA30	CS2 CA30
SiO_2	68.18	66.65	-	63.55	-	61.87	-	-	64.62	43.07
CaO	31.82	31.90	-	32.07	-	32.16	-	-	32.55	33.17
Al_2O_3	-	1.45	-	4.38	-	5.97	-	-	12.83	23.76
NBO/*T*	1.000	0.975	-	0.924	-	0.900	-	-	0.685	0.606
	SW40	SW40 + 5 wt % Al_2O_3	SW40 + 7.5 wt % Al_2O_3	SW40 + 10 wt % Al_2O_3	SA10*	SAN3*	SAN6	NA	CA	-
SiO_2	61.60	58.52	56.98	55.44	90.00	87.00	84.00	-	-	-
CaO	38.40	36.48	35.52	34.56	-	-	-	-	35.48	-
Na_2O	-	-	-	-	-	3.00	6.00	37.81	-	-
Al_2O_3	-	5.00	7.50	10.00	10.00	10.00	10.00	62.19	64.52	-
NBO/*T*	1.336	1.122	1.022	0.926	0.394	0.193	0	0	0	-

NBO/T: Nonbridging oxygens per tetrahedral cation (= sum of tetrahedral cations multiplied by 4, subtracted from number of oxygens times 2, and divided into the number of tetrahedral cations).

NS2: $Na_2Si_2O_5$; CS2: $CaSi_2O_5$; NA: $Na_2Al_2O_4$; CA: $CaAl_2O_4$.

NS2NA2.5, etc.: Mole % Al_2O_3 in NS2, etc., added as $Na_2Al_2O_4$ or $CaAl_2O_4$.

**Excess Al^{3+} over Na^+ calculated as network modifier (see text for further discussion).*

quenched melts, respectively). In NS2 quenched melt ($Na_2Si_2O_5$) the coexisting structural units are predominantly those with NBO/Si = 2 ("chain") and 1 ("sheet"). The Raman spectra of NS2 quenched melt do not show evidence of units with a three-dimensional network structure. Mysen *et al.* (1980d) commented, however, that such units must also be present in order to maintain mass-balance. In CS2 quenched melt ($CaSi_2O_5$), no three-dimensional network units are identified from the Raman spectra. Monomers are observed (Virgo *et al.*, 1980). Mass-balance considerations require, however, the presence of structural units that are more polymerized than that of a sheet. It is likely, therefore, that this composition, in fact, contains three-dimensional structural units.

Experimental methods

The starting compositions were made up from spectroscopically pure (Johnson–Matthey) SiO_2, Al_2O_3 and $CaCO_3$ and reagent-grade (Fisher) Na_2CO_3. Approximately 200 mg of each oxide mixture was ground under alcohol for about 1 hr and stored at 110°C before use. About 50-mg aliquots were converted to glass in a vertical quench furnace by quenching the melts on a Pt dish standing in liquid nitrogen. This quenching technique was used to avoid contamination of the sample from conventional quenching media such as H_2O or Hg. The quenching rates were of the order of 500°C/sec over the first 500°–1000°C.

The samples were checked for homogeneity with Raman techniques described by Mysen *et al.*

(1980c,d). All details of the Raman spectroscopic methods were described by Mysen *et al.* (1980d).

Bands of Gaussian line-shape have been fitted inside the high-frequency envelope of the Raman spectra. It was assumed that the background is flat in this frequency region (800–1200 cm^{-1}). The fitting procedure, as also discussed by Mysen *et al.* (1980a,b,d), was carried out with the following considerations in mind. (1) Published data (Virgo *et al.*, 1979, 1980; Mysen *et al.*, 1980d) indicate that within given ranges of bulk NBO/*T* a fixed number of structural units coexist in the quenched melts. The frequencies of their stretch vibrations in Al-free systems are known. Hence, the number of bands and their maximum frequencies within each high-frequency envelope are indicated. (2) As a result of increasing Si(Al) coupling with increasing Al content in a given system, a given stretch band will shift to lower frequency (Brawer and White, 1977; Virgo *et al.*, 1979). (3) Where possible, the bands should be indicated by the form of the cumulative high-frequency envelope. As also discussed in detail below, this requirement could not always be met because increasing Si(Al) coupling of all the stretch bands in the high-frequency envelope results in decreased spectral resolution. (4) After a set of bands has been fitted inside the high-frequency envelope, other vibrations due to the indicated structural units (*e.g.*, rocking and bending in addition to stretching reflected in the high-frequency envelope) were anticipated at lower frequencies. Such bands were matched against those in the high-frequency envelope. (5) The cumulative area of the fitted bands equals that of the high-frequency envelope within statistical uncertainty.

Melts *vs.* quenched melts (glass)

In this study, quenched melts (glass) have been used to obtain structural information on silicate quenched melt. In order to apply the data on glass (quenched melts) to actual melts it is necessary to document that the structural features under consideration are not significantly affected by quenching of the melt to a glass.

Riebling (1968) and M. Taylor *et al.* (1980) found that the anionic units (silicate polymers) in quenched melts with a three-dimensional network structure, such as quenched melt of $NaAlSi_3O_8$ composition, remain the same as a melt is quenched to a glass. Direct experimental proof of structural similarity between melts and glasses on the join Na_2O–SiO_2 was provided by Sweet and White (1969) and Sharma *et al.* (1978). On the basis of this information it is concluded that the structural features of silicate melts that can be discerned with the Raman spectroscopic technique are quenchable, and the results given in this report are therefore applicable to molten silicates.

Results

Quenched melts with three-dimensional network structures

The structure of quenched melts on the join $NaAlSiO_4$–SiO_2 and of compositions $CaAl_2Si_2O_8$ and $KAlSi_3O_8$ has been studied by M. Taylor and Brown (1979a,b) using RDF (radial distribution function) techniques and by Virgo *et al.* (1979) using Raman spectroscopy. These authors agree that such quenched melts have a three-dimensional network structure. In addition, Virgo *et al.* (1979) concluded that quenched melts on joins such as $CaAl_2O_4$–SiO_2, $NaAlO_2$–SiO_2, $NaGaO_2$–SiO_2 and $NaFeO_2$–SiO_2 may contain at least two different three-dimensional structural units. In pure SiO_2 quenched melts these units differ only in Si–O–Si angle (one unit has a maximum at about 120° and the other at about 160°) according to the structural model of Galeener and Mikkelsen (1979) of the vibrational modes in three-dimensional network structures. The two units are manifested in the Raman spectra by the occurrence of two antisymmetric $Si–O^0$ stretch bands (at 1060 and 1190 cm^{-1}). Additional independent support for such a model for SiO_2 quenched melt may be found in high-resolution transmission electron microscopy studies by Gaskell (1975) and Gaskell and Mistry (1975).

The other end member on aluminate–silica joins is of the type $MAlO_2$ or MAl_2O_4. Quenched melts of $CaAl_2O_4$ composition can be quenched to a clear glass from 1650°C. The unpolarized spectrum of this quenched melt composition can be compared with that of crystalline $CaAl_2O_4$ (crystallized at 1300°C for 20 hr) in Figures 1A and 1B (see Table 2 for detailed Raman data). The spectrum of molten $CaAl_2O_4$ composition consists of a depolarized band near 770 cm^{-1}, a polarized, very strong band near 540 cm^{-1} and two polarized bands that occur as shoulders near 430 and 525 cm^{-1}. The two major bands in crystalline and glassy $CaAl_2O_4$ occur at the same frequency and have similar polarization characteristics. It should be emphasized, however, that this similarity is not proof of structural similarity as there are pronounced differences between the local ordering in glassy materials and the long-range order in crystals.

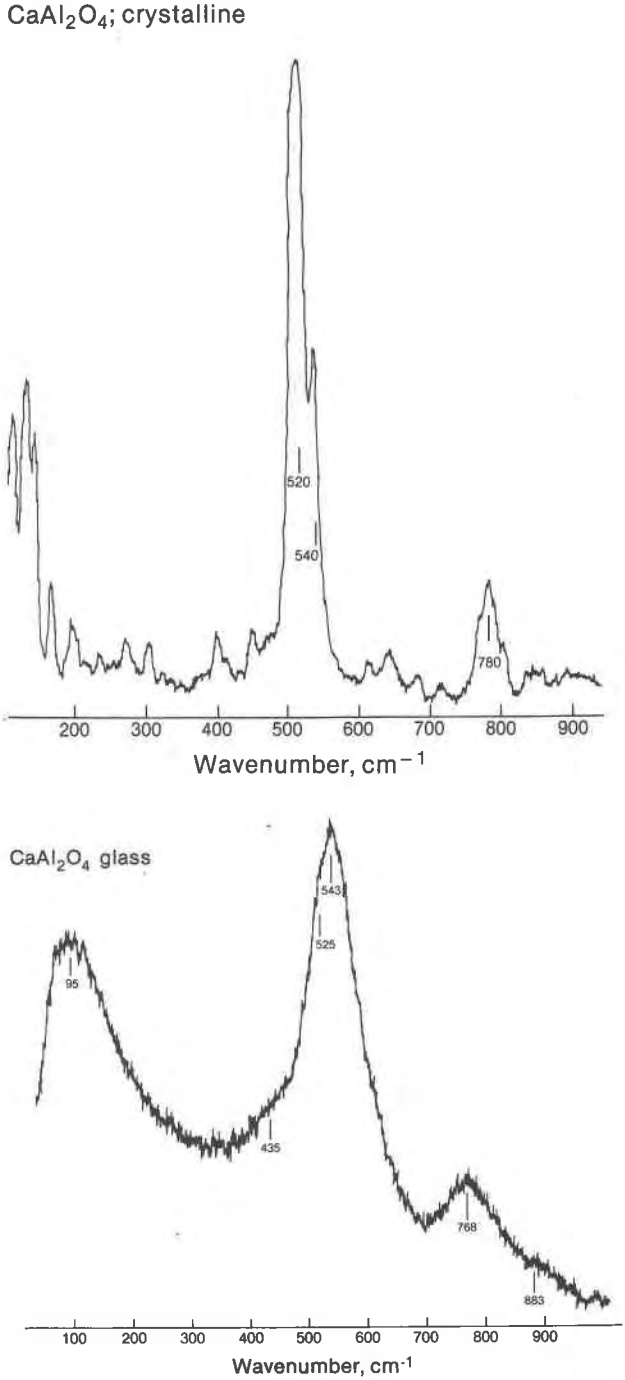

Fig. 1. (A) Unpolarized Raman spectrum of crystalline $CaAl_2O_4$. (B) Unpolarized Raman spectrum of quenched $CaAl_2O_4$ melt.

Table 2. Raman data on melts in the system Na_2O–CaO–Al_2O_3–SiO_2

Comp.	Wavenumber, cm^{-1}												
SiO_2	430 s,p	483 s,p	–	–	595 w,p	–	790 m	–	–	1059 w	–	1188 m	
SAN6	440 s,p	480 (sh)	–	–	587 w,p	–	793 m	–	–	1023 m,p	–	1150 m	
SAN3	431 s,p	483 (sh)	–	–	590 m,p	–	793 m	–	943 w,p	1045 m	1120 w,p	1177 m	
SA10	430 s,p	483 s,p	–	–	600 m,p	m	793 w,p	m	950 mw,p	1052 m	1117	1190	
CA	435 (sh)	–	525 (sh)	543 s,p	–	768 mw	–	883	–	–	–	–	

Abbreviations: s, strong; m, medium; w, weak; mw, medium to weak; p, polarized; (sh), shoulder. Abbreviations of compositions as in Table 1. Uncertainties: 5-10 cm^{-1} except for shoulders, which are 15-20 cm^{-1}.

The major spectral features of glassy $CaAl_2O_4$ (Fig. 1B) may be interpreted with the aid of structural data on glassy SiO_2 and crystalline $CaAl_2O_4$ and the polarization characteristics of the Raman bands. The force constants of Al–O bonds are lower than those of analogous Si–O bonds (Brawer and White, 1977). The frequencies of Raman bands corresponding to the Al–O bonds will therefore be lower than those of analogous Si–O bonds. The three-dimensional structure of $CaAl_2O_4$ quenched melt is reflected in the 768 cm^{-1} band, which may be due to Al–O^0 antisymmetric stretching (the symbols -0^0, -0^- and O^{2-} are defined by Brawer and White (1977) and also by Mysen *et al.* (1980d)). The very strong polarized band near 540 cm^{-1} is probably due to symmetric Al–O^0 stretching. There may also be a very weak band near 880 cm^{-1} (Fig. 1B), which may be assigned to a second antisymmetric Al–O^0 stretch band analogous to the assignment of the antisymmetric Si–O^0 stretch band at 1190 cm^{-1} in SiO_2 glass also found in three-dimensional aluminosilicate quenched melts (Fig. 2).

On the basis of the above discussion and the data on joins such as $NaAlO_2$–SiO_2 and $CaAl_2O_4$–SiO_2 (Virgo *et al.*, 1979; Mysen *et al.*, 1980d), it is concluded that silicate quenched melts on these joins retain a three-dimensional network structure with two different structural units that differ in Si(Al)–O–Si(Al) angle and probably Al content. There is no evidence for Al^{3+} as a network modifier in quenched melts with Na/Al = 1.

Quenched melts in the system Na_2O-Al_2O_3-SiO_2 with Na/Al less than 1

It has been suggested (*e.g.*, Day and Rindone, 1962a,b; Riebling, 1964, 1966; Wood and Hess, 1980; Mysen *et al.*, 1980d) that if Al^{3+} is added to quenched melts in excess of that which may be charge-balanced with metal cations such as Na^+ or Ca^{2+}, the extra

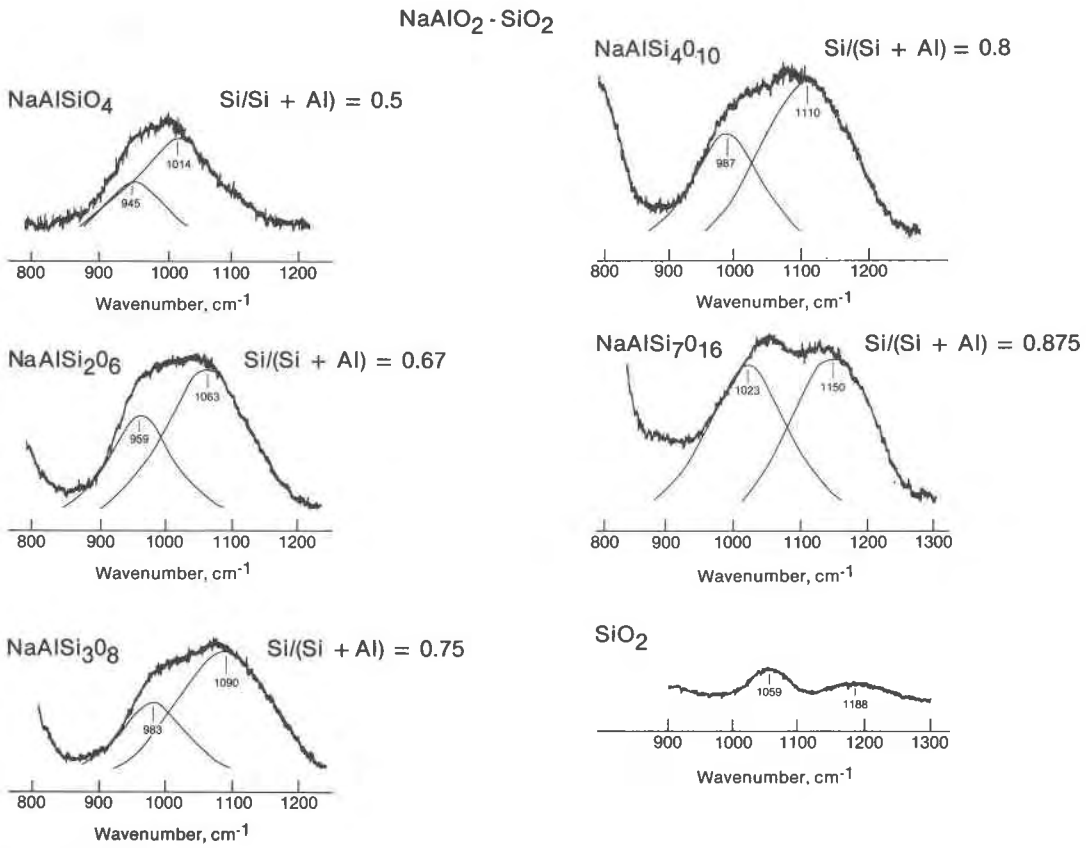

Fig. 2. Unpolarized Raman spectra of melts on the join $NaAlO_2$–SiO_2 (from Mysen *et al.*, 1980d).

aluminum may not be in tetrahedral coordination. Lacey (1963), on the other hand, suggested that AlO_6 octahedra will not be energetically stable and proposed the AlO_6-tricluster concept as an alternative structure. In that model, Al^{3+} remains in tetrahedral coordination without local charge-balance, and no nonbridging oxygens will be formed.

In melts with Al^{3+} in octahedral coordination the assignments of bands in Raman spectra due to oxygen bonds involving nonbridging oxygens can be made on a basis similar to the assignment of nonbridging oxygens in depolymerized silicate melts (Brawer and White, 1975, 1977; Virgo *et al.*, 1980; Mysen *et al.*, 1980d). Furthermore, on the basis of studies of melts on the join Na_2O–SiO_2 with 5 mole % Na_2O or less in solution and the discussion by Lucovsky (1979a,b) of the spectroscopic response to defects in SiO_2 melt, it may be estimated that if more than about 1% of the oxygens in the melts is nonbridging, symmetric stretch bands reflecting such units may be discerned in the spectra.

The melt compositions SA10, SAN3 and $NaAlSi_7O_{16}$ (SAN6; Na/Al = 1) (Table 1) were prepared to evaluate the proposed roles of Al^{3+} in silicate melts as a function of availability of charge-balancing cations. The high-frequency envelope of the Raman spectra of these melts is shown in Figure 3 (see also Table 2). The portion of the spectra below about 800 cm^{-1} is not significantly different from that of quenched SiO_2 melt (Table 2). A significant portion of the melt structures is probably, therefore, three-dimensional (cf. Figs. 2 and 3; see also Table 2). In quenched SA10 melt, there are, however, two additional bands in the high-frequency envelope (near 950 and 1100 cm^{-1}; Fig. 3). Both bands are polarized and become less intense as 3 wt.% Na_2O is added to the melt (as in SAN3 melt; Fig. 3).

In quenched SA10 melt, the two strongest bands (at 1050 and 1190 cm^{-1}) are depolarized and are probably the two antisymmetric stretch bands also found in quenched SiO_2 melt. The frequencies and polarization characteristics of the two bands near 950 and 1100 cm^{-1} are nearly identical with those in melts on the join Na_2O–SiO_2 (Brawer and White,

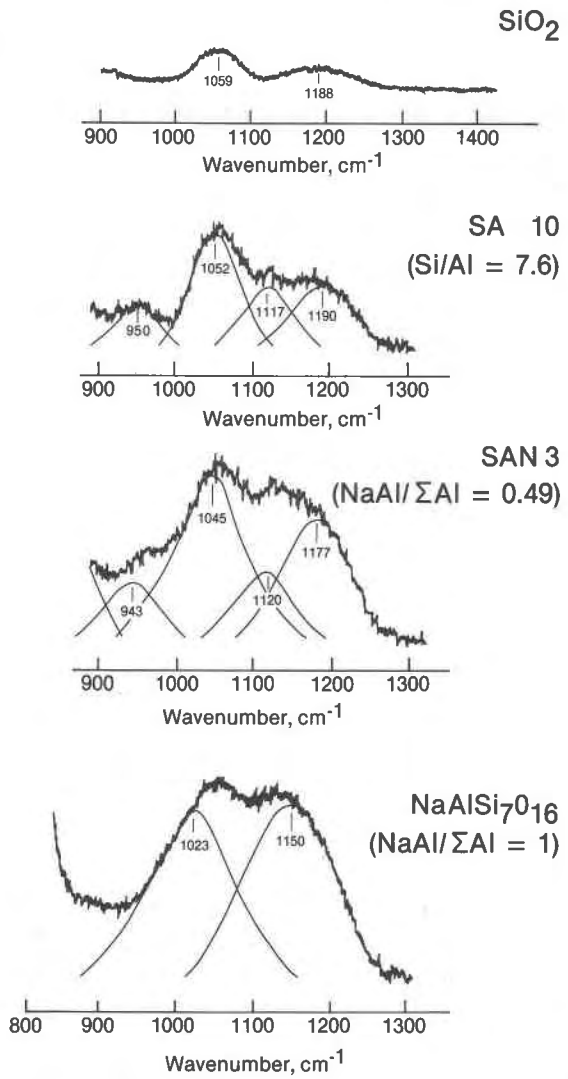

Fig. 3. Unpolarized Raman spectra of melts on the join SAN6–SA10.

1975; Verweij, 1979a,b; Mysen *et al.*, 1980d) and may be due to symmetric $^{-}$O–Si–O^{-} and $^{-}$O–Si–O^{0} stretch vibrations (corresponding to structural units with, respectively, 2 and 1 NBO/Si).

Additional evidence for the absence of tetrahedrally coordinated Al^{3+} is that there is no indication of Si(Al) coupling of any of the bands in the high-frequency envelope of the spectrum of SA10 melt (Fig. 3). Furthermore, there is no evidence of new bands at lower frequencies (near 850 and 770 cm^{-1}), bands that could indicate the presence of aluminum–oxygen clusters with Al^{3+} in tetrahedral coordination. It is concluded, therefore, that all Al^{3+} in quenched SA10 melt (90 wt.% SiO_2 and 10 wt.% Al_2O_3) is a network modifier.

In composition SAN3, sufficient Na^{+} is present to charge-balance approximately half of the Al^{3+} (Table 1). In the Raman spectrum of this composition (Fig. 3) the frequencies of the two Si–O^{0} antisymmetric stretch bands are slightly lower than in SiO_2 and SA10 melts (Fig. 3; see also Table 2). This observation indicates some Si(Al) coupling with Al^{3+} in tetrahedral coordination. On the basis of the data of Virgo *et al.* (1979), the frequencies of the two antisymmetric Si(Al)–O^{0} stretch bands in the spectrum of SAN3 melt indicate that Si/(Si+Al) cannot be significantly less than 0.95 in the three-dimensional network units. This value compares with Si/(Si+Al) = 0.93 in the bulk SAN3 composition (Tables 1 and 2; Figs. 1–3). It is concluded, therefore, that some of the Al^{3+} is not in tetrahedral coordination. This suggestion is substantiated by the persistence of the two bands near 950 and 1100 cm^{-1} in the Raman spectrum of quenched SAN3 melt (Fig. 3). These two bands also indicate that nonbridging oxygens are present. The intensities of these bands (and in particular that of the 1100 cm^{-1} band) have diminished relative to the overall intensity of the high-frequency envelope. The proportion of nonbridging oxygens in quenched SAN3 melt is therefore less than in quenched SA10 melt. The overall similarity of the Raman spectra of the two melts with excess Al^{3+} over Na^{+} indicates that the same structural units occur in both melts. Their porportions differ, however, as a function of Na/Al ratio.

The spectrum of SAN6 melt (Na/Al = 1) is similar to that of quenched SiO_2 melt (see also Mysen *et al.*, 1980d) in that no bands indicative of nonbridging oxygens are found (Fig. 3; see also Table 1). The frequencies of the two antisymmetric stretch bands in the high-frequency envelope (at 1023 and 1150 cm^{-1}, respectively) are lower than in SAN3 melt and also lower than in quenched SiO_2 melt. Thus more extensive Si(Al) coupling in the three-dimensional network is indicated.

On the basis of the above discussion, it is concluded that Al^{3+} without metal cations for local charge-balance do not form AlO_6-triclusters with Al^{3+} in tetrahedral coordination as suggested by Lacey (1963). The existence of such structural units would result in Al–O^{0} stretch vibrations, which are not observed. Furthermore, no nonbridging oxygens will be created if AlO_6-triclusters were formed. However, Si(Al)–O^{-} vibrations occur. Instead, the Raman spectra of SA10 of SAN3 quenched melt indicates

that such Al^{3+} is a network-modifier. In SA10 melt, all Al^{3+} is a network-modifier. In SAN3 quenched melts, approximately 50% of the Al^{3+} is a network-modifier. In SAN3 quenched melts, approximately 50% of the Al^{3+} is charge-balanced with Na^+ thus reducing the proportion of nonbridging oxygen created by Al^{3+}.

Melts on the join $Na_2Si_2O_5$–$NaAlO_2$

In order to study the distribution of $NaAl^{4+}$ complexes between structural units with NBO/T = 0, 1 and 2, $Na_2Al_2O_4$ was added in amounts up to 40 mole % calculated as Al_2O_3. The compositions of the starting materials are given in Table 1. All the samples on this join were prepared at 1400°C.

The Raman spectrum of aluminum-free $Na_2Si_2O_5$ (Fig. 4; see also Table 3) has been described and interpreted previously (Brawer and White, 1975; Verweij, 1979b; Mysen *et al.*, 1980d), and only a summary of those conclusions is presented. The very weak band near 1175 cm^{-1} is due to antisymmetric stretching of bridging oxygen bonds in three-dimensional network units. The very strong, sharp and polarized 1095 cm^{-1} band is due to $^-O–Si–O^0$ symmetric stretching, and the relatively weak 950 cm^{-1} band is due to symmetric $^-O–Si–O^-$ stretching. The 1050 cm^{-1} band occurs in all melts with bridging oxygens and is assigned to antisymmetric stretching of bridging oxygens in any structural unit with such bonds. This band cannot be used to discriminate between individual types of structural units (Furukawa and White, 1980; Mysen *et al.*, 1980d). The weak 773 cm^{-1} band is an oxygen-bending motion. The 573 cm^{-1} band is a rocking motion of bridging oxygens in structural units that contain nonbridging oxygen (Brawer and White, 1977; Brawer, 1975; Lazarev, 1972). Its frequency changes from slightly less than 600 cm^{-1} for structural units with NBO/Si about 1 to slightly less than 700 cm^{-1} for dimers (Mysen *et al.*, 1980d). The band is probably a composite in melts with several types of structural units. Consequently, the band tends to be asymmetric with a maximum near the frequency of the vibration of the predominant unit in the melt.

Addition of Al^{3+} to the structural units in melts result in a continuous downward shift of the frequencies of characteristic stretch vibrations as a function of increasing Al content of the relevant structural units (Brawer and White, 1977); Virgo *et al.*, 1979). If Al^{3+} is a network modifier, no such effect will be observed. Instead, the intensity of the Raman band stemming from structural units with nonbridging oxygens will increase. If Al^{3+} clusters into Al-rich units with Al^{3+} in tetrahedral coordination, new bands below 800 cm^{-1} will result. Alternatively, if there already are bands in the same region, the composite band intensity will increase. For example, if clusters of tetrahedrally coordinated Al^{3+} like that found in quenched $CaAl_2O_4$ melt are formed, the resultant depolarized band near 770 cm^{-1} will add to the 770 cm^{-1} Si–O deformation band already there. It is important in this context to remember that these latter two spectral effects should occur together in order for such an interpretation to be viable.

In overall appearance the Raman spectra of NS2 melt with up to 7.5 mole % Al_2O_3 (added as $Na_2Al_2O_4$) resemble those of Al-free, NS2 quenched melt (Figs. 4B-D; see also Table 3). Neither the 1095 cm^{-1} band nor the 940 cm^{-1} band appears affected within experimental uncertainty. It is suggested, therefore, that neither the sheet nor the chain unit in this melt contains a significant amount of Al^{3+}. The 1050 cm^{-1} band in pure NS2 melt shifts to lower frequency with higher Al content. It is concluded, therefore, that some Si(Al) coupling of bridging oxygen bond vibrations has occurred in at least some of the structures in the melt. If this coupling resulted from the formation of Al-bearing chain and sheet units, the frequencies of the 1095 and 940 cm^{-1} bands should also have shifted down, but they have not done so (Fig. 4). The shift of the 1050 cm^{-1} band must therefore be due to Al^{3+} entering the three-dimensional network units in the melt. If so, the band found near 1170 cm^{-1} in pure NS2 melt will shift downward. The band will fall beneath the high-frequency limb of the 1095 cm^{-1} band and is not easily resolved. The buildup of a shoulder near 500 cm^{-1} may reflect an increased proportion of three-dimensional network units in the melt.

The 570 cm^{-1} band in pure NS2 melt is split into a sharp, polarized band near 550 cm^{-1} and a shoulder near 590 cm^{-1} as 2.5 mole % Al_2O_3 is added to the melt (Fig. 4B). At the same time, the intensity of the band near 770 cm^{-1} has increased. It is possible, therefore, that aluminate clusters have been formed in addition to some Al^{3+} randomly mixed with Si^{4+} in the three-dimensional network units.

It is noted that the frequency of the 1020 cm^{-1} band in NS2NA2.5 is the same in NS2NA5 quenched melts. This observation is interpreted to mean that the bulk Si/(Si+Al) of the silicate anionic structural units has not been affected. In order for this to happen, the proportion of three-dimensional structural units in the melt must have increased rela-

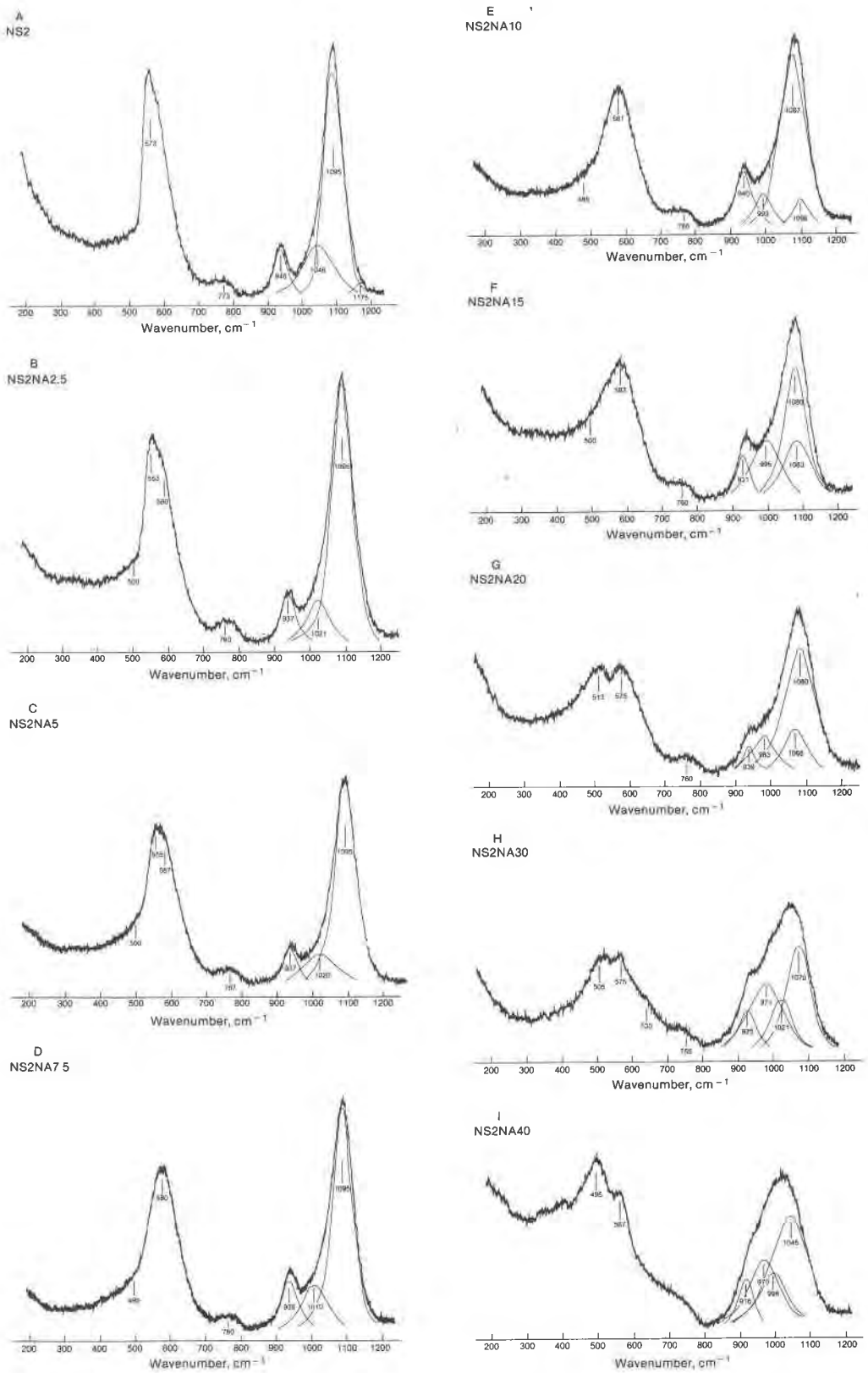

Fig. 4. Unpolarized Raman spectra of quenched melts on the join $Na_2Si_2O_5$–$NaAlO_2$ (symbols as in Table 1).

Table 3. Raman data on melts on the join $Na_2Si_2O_5$–$NaAlO_2$

Comp.	Wavenumber, cm^{-1}								
NS2	-	-	573 s,p	-	773 vw	945 m,p	1046 m	1095 s,p	1175 vw
NS2NA2.5	500 (sh)	553 s,p	590 (sh)	-	760 w	937 m,p	1021 m	1095 s,p	n.d.
NS2NA5	500 (sh)	550 s,p	587 (sh)	-	767 vw	937 w,p	1020 mw	1095 s,p	n.d.
NS2NA7.5	495 (sh)	-	580 s,p	-	760 vw	935 mw,p	1010 mw	1095 s,p	n.d.
NS2NA10	485 (sh)	-	581 ms,p	-	765 vw	940 mw,p	993 mw	1087 s,p	1098 w
NS2NA15	500 (sh)	-	583 ms,p	-	760 vw	931 w,p	995 m	1080 ms,p	1083 m
NS2NA20	513 m,p	-	575 m,p	-	760 vw	939 w,p	983 mw	1080 ms,p	1068 m
NS2NA30	505 m,p	-	575 m,p	630 (sh)	755 vw	925 mw,p	971 ms	1070 ms,p	1021 m
NS2NA40	495 ms,p	-	567 mw,p	-	-	916 mw,p	970 m	1045 ms,p	995 m

Abbreviations: s, strong; ms, medium to strong; m, medium; mw, medium to weak; w, weak; vw, very weak; p, polarized; (sh), shoulder; n.d., not determined. Uncertainties as in Table 2. Other notations as in Table 1.

tive to the structural units with NBO/Si = 1 and 2 (none of which appears to contain any Al^{3+}). This conclusion is likely inasmuch as addition of $Na_2Al_2O_4$ to the melt results in a bulk decrease of NBO/T of the melt. An alternative interpretation is that the proportion of three-dimensional aluminate units has increased. This interpretation is unlikely, however, because the intensities of the 770 and 550 cm^{-1} bands have not increased. The antisymmetric stretch band at 1020 cm^{-1} with 5 mole % Al_2O_3 has shifted further down with 7.5 mole % Al_2O_3 in solution (to 1010 cm^{-1}; Fig. 4D). The latter observations indicate, therefore, that the three-dimensional network unit of the melt has become even more aluminous, whereas the silicate units with nonbridging oxygens remain Al-free.

The strong, polarized 550 cm^{-1} band found in NS2NA2.5 and NS2NA5 quenched melts can no longer be discerned in NS2NA7.5 quenched melt, although the 760–770 cm^{-1} band is still present (Fig. 4D). The latter band on its own does not indicate aluminate complexes, however. It is concluded, therefore, that the proportion of three-dimensional aluminate complexes is diminished and that random mixing of Si^{4+} and Al^{3+} in the three-dimensional structural units is predominant.

The spectrum of quenched NS2NA10 melt is shown in Fig. 4E (see also Table 3). The portion of the spectrum below about 800 cm^{-1} is similar to that of NS2NA7.5 quenched melt (Fig. 4D). The high-frequency envelope is, however, somewhat altered. The 940 cm^{-1} band remains in the same position. Thus insignificant Al^{3+} in the structural unit with NBO/T = 2 is indicated. The 1095 cm^{-1} band ($^-$O–Si–O^0 symmetric stretch) may have shifted to slightly lower frequency (1087 cm^{-1}). It is now also possible to insert the fourth band (Si–O^0 antisymmetric stretching in a three-dimensional network) into the high-frequency envelope. Its frequency is about 80 cm^{-1} less than that in pure NS2 melt (about 1170 cm^{-1}). As also argued for the composition NS2NA7.5, there are no indications in this spectrum (Fig. 4E) that aluminate complexes are present.

The spectra of quenched NS2NA15 and NS2NA20 melts (Figs. 4F and G; see also Table 3) resemble that of NS2NA10 (Fig. 4E) except that all the bands in the high-frequency envelope have shifted to lower frequencies, resulting in an overall broadening of the envelope. The rate of change of the frequency of the antisymmetric stretch band of Si–O^0 (or strictly Si(Al)–O^0 as there is Al^{3+} in the structure) has shifted the most of all the bands. This result indicates that the rate of decrease of Si/(Si+Al) in this structural unit is faster than in the other structural units (with NBO/T = 1 and 2, respectively). The 940 cm^{-1} band may also have shifted slightly in this composition relative to those with less aluminum (Fig. 4). The portion of the spectrum below 800 cm^{-1} is unaffected. Thus, there are no other changes in the structure of the melt.

The spectrum of NS2NA20 melt also indicates that the intensity of the $^-$O–Si–O$^-$ symmetric stretch band (near 940 cm^{-1}) has decreased and that of the Si(Al)–O^0 antisymmetric stretch band near 1070 cm^{-1} has increased relative to the intensity of the entire high-frequency envelope (see Fig. 4). These intensity changes reflect the increased overall degree of polymerization of the melt as $NaAlO_2$ is added to NS2 melt. The significantly increased degree of polymerization is also beginning to show in the lower portion of the spectrum of NS2NA20 melt (Fig. 4G). The band near 570 cm^{-1} is now split into two bands (Fig. 4G), one near 575 and one near 515 cm^{-1}. Both bands are polarized. A polarized band near 500 cm^{-1} is also observed in melts of $CaAl_2Si_2O_8$ and $NaAlSi_3O_8$ compositions (Virgo *et al.*, 1979). The 515 cm^{-1} band probably corresponds to the Si(Al)–O^0 rocking band in three-dimensional network structures. The possible presence of such a band in melts with less Al may be indicated by the increased broadness of the

570 cm^{-1} band with increasing Al content up to 15 mole % (added as $Na_2Al_2O_4$).

The spectrum of NS2NA30 (30 mole % Al_2O_3 added as $Na_2Al_2O_4$) resembles that of NS2NA20 (Figs. 4G and H). The evolution to lower frequencies in the high-frequency envelope has continued, the rate of change being greatest for the antisymmetric Si(Al)–O^0 stretch band and slowest for the symmetric $^{-1}$O–Si(Al)–O^{-1} stretch band. The two separate bands near 575 and 505 cm^{-1} persist, and it appears that the 505 cm^{-1} band has grown relative to the 575 cm^{-1}, an evolution that would be expected as three-dimensional network structural units become more important relative to depolymerized units in the melt. A shoulder has also developed on this low-frequency double band. The shoulder is near 630 cm^{-1} (Fig. 4H). The 630 cm^{-1} band is polarized and occurs at the position where a band characteristic of deformation of the bridging oxygen in chain units can be found (Etchepare, 1972; Lazarev, 1972; Brawer and White, 1975; Virgo *et al.*, 1980; Mysen *et al.*, 1980c,d). In such systems the band is also polarized. Inasmuch as there are symmetric stretch bands indicative of the presence of a structural unit with NBO/T = 2 in this melt, the appearance of the band near 630 cm^{-1} would be expected.

The most aluminous composition in the system $Na_2Si_2O_5$–$NaAlO_2$ is NS2NA40 (40 mole % Al_2O_3 added as $Na_2Al_2O_4$). The high-frequency envelope of the spectrum from this composition (Fig. 4I) has lost most of the structure found in the less aluminous samples. The fitting of the four bands was simply done to show how four bands may be fitted to this envelope, the frequencies of which are in positions consistent with the evolution indicated by the less aluminous samples. In the low-frequency portion of the spectrum it is noted that the intensity of the 500 cm^{-1} band relative to that of the 570–580 cm^{-1} band has increased even further. Thus it is indicated that three-dimensional network units in the melt have become even more dominant.

The frequency changes of the stretch bands in the high-frequency envelope as a function of $Na_2Al_2O_4$ content has been summarized in Figure 5. It can be seen from these data that the rate of change of the antisymmetric Si(Al)–O^0 stretch band is much more rapid than that of the symmetric $^{-}$O–Si(Al)–O^0 stretch band and that the rate of change of the $^{-}$O–Si–O^{-} symmetric stretch band is almost zero. These observations indicate, therefore, that when Na^+ and Al^{3+} form $NaAl^{4+}$ complexes in tetrahedral coordination, the aluminate complexing is more pronounced

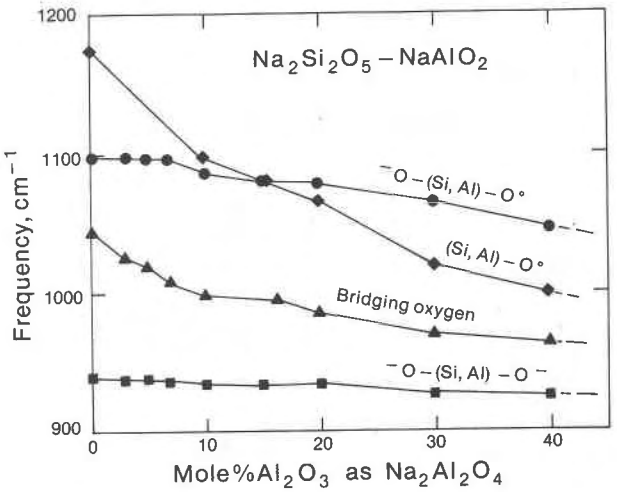

Fig. 5. Frequency change of important Raman bands in the system $Na_2Si_2O_5$–$NaAlO_2$ as a function of Al content (mole % Al_2O_3 on the basis of 5 oxygens).

in the three-dimensional network structure than in the sheet structure. Only a very small proportion of Al^{3+} occurs in the chain.

Melts on the join $Na_2Si_2O_5$–$CaAl_2O_4$

$CaAl_2O_4$ was added to NS2 melt in order to evaluate whether the presence of Ca^{2+} in the melt would affect the preference of Al^{3+} for the structural units in the melt. The spectrum of NS2CA2.5 (Fig. 6A; see also Table 4) is nearly identical with that of NS2NA2.5 (Fig. 4A). It is concluded, therefore, that the addition of 2.5 mole % Al_2O_3 as $CaAl_2O_4$ to NS2 melt has the same effect on the melt as the addition of Al_2O_3 as $Na_2Al_2O_4$.

The spectrum of NS2CA5 melt (Fig. 6B) resembles those of NS2CA2.5 and NS2NA5 (Figs. 4B and 6A). It differs from the latter, however, in that the 550–770 cm^{-1} band combination is no longer obvious in the calcic system, whereas it is still present in NS2NA5. There is, therefore, an insignificant amount of aluminate in melt of NS2CA5 composition. The 940 and 1100 cm^{-1} bands are not affected; thus it is indicated that all the aluminum is in the three-dimensional network structure.

The addition of 10 mole % Al_2O_3 as $CaAl_2O_4$ (Fig. 6C) causes all the bands in the high-frequency envelope to shift to slightly lower frequencies, and the 580 cm^{-1} band becomes broader. It is concluded, therefore, that the addition of 10 mole % Al_2O_3 as $CaAl_2O_4$ results in a more even distribution of Al^{3+} between the structural units than the addition of Al^{3+} as $Na_2Al_2O_4$. The types of anionic units are the same.

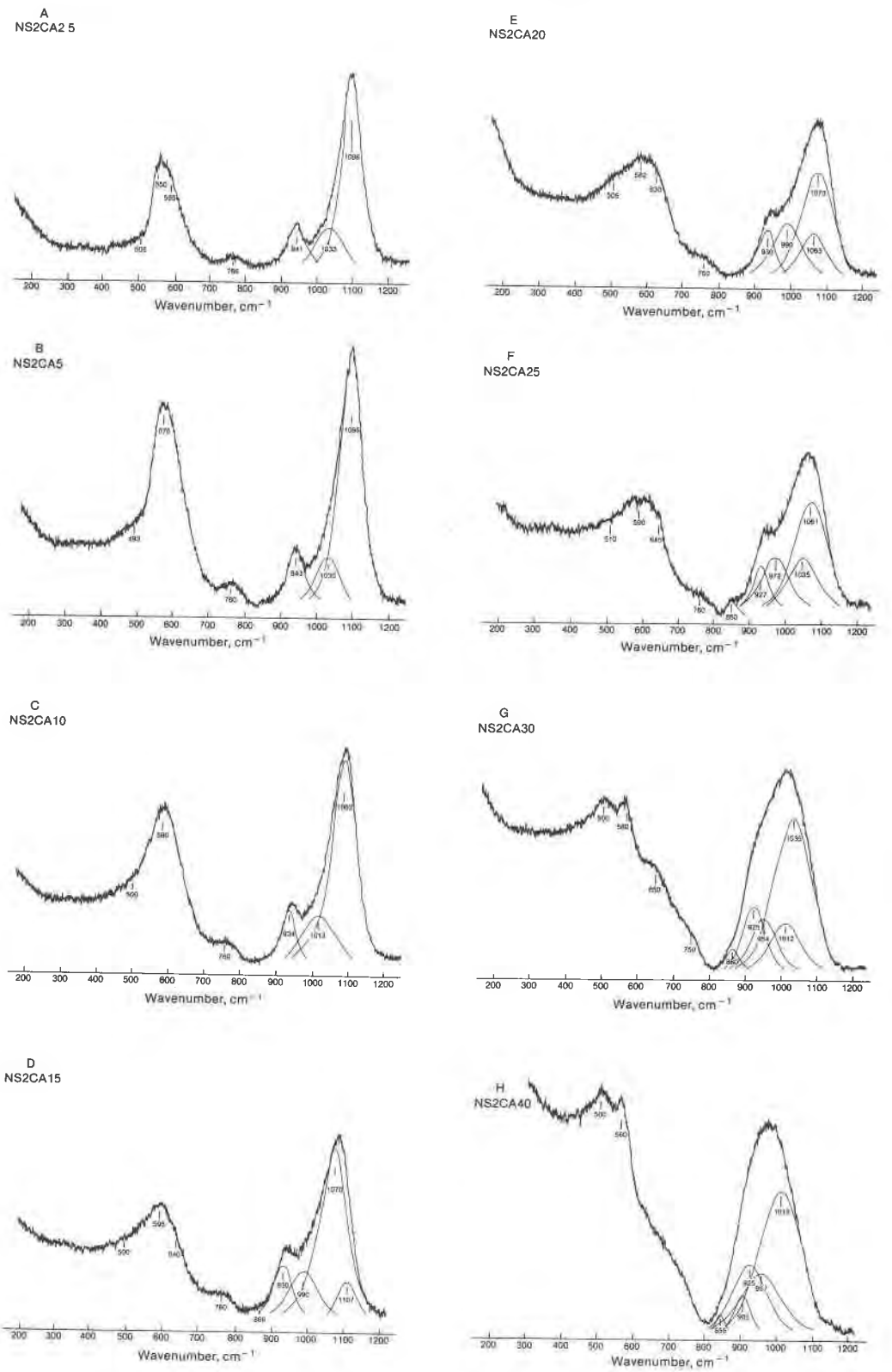

Fig. 6. Unpolarized Raman spectra of melts on the join $Na_2Si_2O_5$–$CaAl_2O_4$ as a function of Al content (symbols as in Table 1).

Table 4. Raman data on melts on the join $Na_2Si_2O_5$–$CaAl_2O_4$

Comp.	Wavenumber, cm^{-1}									
NS2CA2.5	505 (sh)	550 ms,p	585 (sh)	766 vw	–	–	941 mw,p	1033 m	1098 s,p	n.d.
NS2CA5	493 (sh)	–	576 s,p	–	760 vw	–	943 mw,p	1030 mw	1095 s,p	n.d.
NS2CA10	500 (sh)	–	580 s,p	–	760 vw	–	934 mw,p	1013 m	1082 s,p	n.d.
NS2CA15	500 (sh)	–	595 m,p	640 (sh)	760 vw	866 vw	930 mw,p	990 m	1070 s,p	1107 w
NS2CA20	505 w,p	–	582 m,p	630 (sh)	760 vw	–	930 mw,p	990 m	1073 ms,p	1063 m
NS2CA25	510 (sh)	–	590 m	645 (sh)	760 vw	850 vw	927 mw,p	972 m	1061 ms,p	1035 m
NS2CA30	500 mw,p	–	580 mw,p	650 (sh)	750 (sh)	860 vw,p	925 mw,p	954 m,ms,p	1035 m	1012
NS2CA40	500 m,p	–	560 m,p	–	–	855 vw	905 w,p	925 m	1012 ms,p	957 m

Abbreviations as in Tables 1 and 3.

Whether the more even Al distribution is due to a different effect of Ca^{2+} as a network modifier or whether aluminum is in fact charge-balanced by Na^+ cannot be determined from these data.

With 15 mole % Al_2O_3 added as $CaAl_2O_4$ (NS2CA15; Fig. 6D), the highest-frequency, antisymmetric stretch band (reflecting the three-dimensional network unit) can be discerned. It is noted that its frequency is significantly higher than that of the analogous band in NS2NA15 (1107 and 1088 cm^{-1}, respectively; see Tables 3 and 4). It is suggested that this difference exists because the Si/(Si+Al) in the three-dimensional network units is higher in NS2CA15 than in NS2NA15 melt. On this basis, it is concluded that Al^{3+} is more evenly distributed between the structural units in the former system. The diminished intensity of the 580–590 cm^{-1} band relative to that of the high-frequency envelope may indicate that the proportion of structural units with $NBO/T = 1$ has decreased, as would be expected as $CaAl_2O_4$ is added to the system.

The spectrum of quenched NS2CA20 melt (Fig. 6E) is a natural evolution of that of less aluminous samples and also matches the evolution in the sodic system (Fig. 4G). One notable difference between the two systems, however, is that the intensity ratio of the 500–580 cm^{-1} band in NS2NA20 (Fig. 4G) is considerably greater than in NS2CA20 (Fig. 6E). This observation indicates that the proportion of three-dimensional network units relative to sheet units is greater in the system NS2NA than in NS2CA.

Aside from the appearance of a new small band near 850 cm^{-1}, and a further decrease in the frequencies of all the stretch bands, the spectrum of NS2CA25 (Fig. 6F) resembles that of NS2CA20. The assignment of the 850 cm^{-1} band is open to some question. It cannot be assigned to aluminate complexes as its frequency is too high. The band is polarized. It is suggested, therefore, that this is a symmetric stretch vibration. This band may be another depolymerized, structural unit with a large proportion of Al^{3+}.

The spectra of NS2CA30 and NS2CA40 quenched melts (Figs. 6G and H; see also Table 4) are poorly resolved. The bands in the high-frequency envelope are fitted so that they are consistent with the interpretation of the lower frequency bands and with all the other spectra in the system.

The rate of change of the frequencies of the stretch bands in the system $Na_2Si_2O_5$–$CaAl_2O_4$ is summarized in Figure 7. This summary shows a general trend similar to that of the system $Na_2Si_2O_5$–$NaAlO_2$, except that the slope of the curve for the antisymmetric stretch band is more gentle and the slopes of the curves for the ^-O–Si(Al)–O^0 and ^-O–Si(Al)–O^- symmetric stretch bands are somewhat steeper. These observations indicate a more even distribution of Al^{3+} in the system involving both Na^+ and Ca^{2+} than in the system where Na^+ is the only metal cation.

Melts in the system $CaSi_2O_5$–$CaAl_2O_4$

The compositions in the system $CaSi_2O_5$–$CaAl_2O_4$ (CS2–CA) represent a further evolution in the study of the influence of metal cations on Al^{3+} distribution

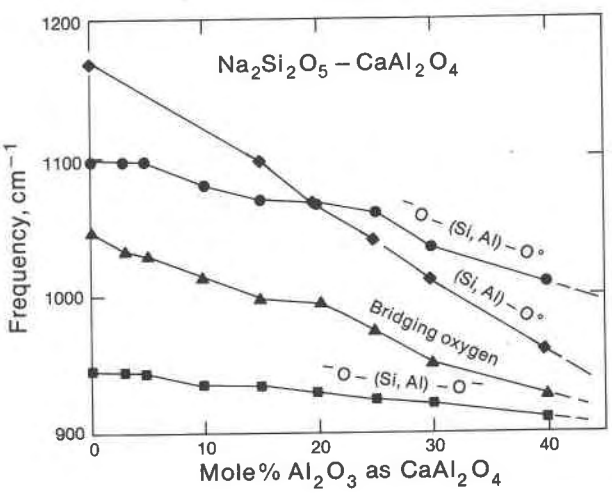

Fig. 7. Frequency change of important Raman bands in the system $Na_2Si_2O_5$–$CaAl_2O_4$ as a function of Al content (mole % Al_2O_3 on the basis of 5 oxygens).

in systems involving depolymerized structural units. In this case, Ca^{2+} is both the charge-balancing cation in the aluminate and the network-modifying cation in the melts.

The structure of CS2 quenched melt has been discussed by Virgo *et al.* (1979) and Mysen *et al.* (1980d). In those studies, it was concluded that the disilicate composition (NBO/Si = 1) is on the boundary between melts where the structure may be described with equation 2 or 3. In the sodium disilicate, the coexisting anionic units have, on the average, NBO/Si = 2, 1 and 0. The spectrum of quenched CS2 melt (Fig. 8; see also Table 5) shows several similarities to that of quenched NS2 melt (Fig. 4A) but

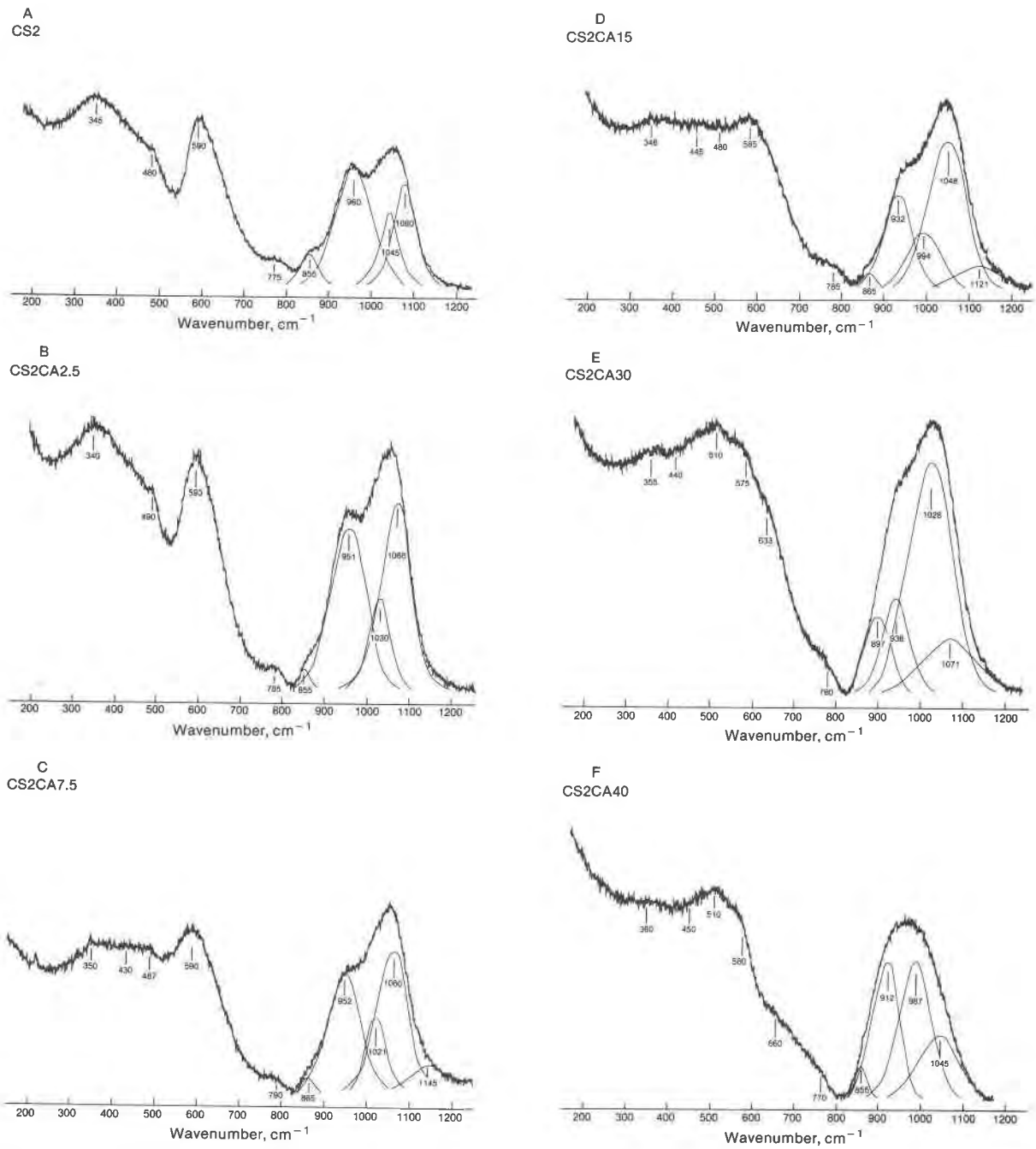

Fig. 8. Unpolarized Raman spectra of quenched melts on the join $CaSi_2O_5$–$CaAl_2O_4$ as a function of Al content (symbols as in Table 1).

Table 5. Raman data on melts on the join $CaSi_2O_5$–$CaAl_2O_4$

Comp.	Wavenumber, cm^{-1}										
CS2	345 mw	–	480 (sh)	590 ms,p	–	775 vw	855 vw,p	960 ms,p	1045 m	1080 ms,p	n.d.
CS2CA2.5	340 mw	–	490 (sh)	593	– vw	785 vw,p	855 s,p	951 ms,p	1030 m	1068 ms,p	n.d.
CS2CA7.5	350 (sh)	430 vw	487 (sh)	590 m,p	–	790 vw	865 vw,p	952 s,p	1021 m	1060 s,p	1145 w
CS2CA15	345 (sh)	445 vw	480 vw	585 w,p	–	785 vw	865 vw,p	932 m,p	994 m	1048 s,p	1121 mw
CS2CA30	355 vw	440 (sh)	510 mw	575 (sh)	633 (sh)	780 (sh)	–	897 mw,p	938 m	1028 s,p	1071 m
CS2CA40	360 vw	450 (sh)	510 w	580 (sh)	660 (sh)	770 (sh)	–	855 vw,p	912 ms	987 ms,p	1045 m

Abbreviations as in Tables 1 and 3.

also certain differences. The main difference is a weak, polarized band near 855 cm^{-1}. This band appears to be the same one found in more depolymerized melts, where it is assigned to Si–O^{2-} symmetric stretching (Verweij, 1979a,b; Furukawa and White, 1980; Virgo *et al.*, 1979; Mysen *et al.*, 1980d). This band, therefore, may be due to the presence of a small amount of separate SiO_4^{4-} monomers in the melt. The 960, 1080 and 1045 cm^{-1} bands have the same polarization characteristics and otherwise are similar to those at 940, 1095 and 1050 cm^{-1} in quenched NS2 melt, and are given the same assignments (Virgo *et al.*, 1979; Brawer and White, 1977; Furukawa and White, 1980; Mysen *et al.*, 1980d). These assignments are $^-$O–Si–O^- and $^-$O–Si–O^0 symmetric stretching and Si–O^0 antisymmetric stretching. The band at 590 cm^{-1} (Fig. 8A) is analogous to the 570 cm^{-1} band in NS2 quenched melt (Fig. 4A) and is therefore assigned to deformation of bridging oxygen bonds in sheet units. The 345 cm^{-1} band commonly occurs in calcic systems with nonbridging oxygens (Brawer and White, 1977; Mysen *et al.*, 1980c,d). It has been suggested that this band is due to vibrations in Ca-oxygen polyhedra (Brawer and White, 1977). A band near 480 cm^{-1}, when associated with one near 780–800 cm^{-1} and one near 1180 cm^{-1}, has been assigned to rocking motions in a three-dimensional network (Bates *et al.*, 1974; Bell and Dean, 1972; Galeener and Lucovsky, 1976; Lucovsky, 1979a). The 1180 cm^{-1} band appears to be absent in the present spectrum. At least it cannot be easily fitted into the high-frequency envelope. It is likely, however, that it is there for the following reason. The bulk NBO/Si of $CaSi_2O_5$ is 1. The structural units already identified in this melt composition have NBO/Si equal to or greater than 1. Unless there is at least one structural unit with NBO/Si less than 1, the system cannot be mass-balanced. It is suggested, therefore, that there is also a structural unit with NBO/Si near 0 in this system, but that its associated antisymmetric stretch band cannot be separated from other bands in the high-frequency envelope.

The Raman spectrum of CS2CA2.5 does not differ substantially from CS2 (Figs. 8A and B; see also Table 5). There is no indication that aluminate complexes occur in this melt in contrast to NS2CA2.5 and NS2NA2.5 melts (Figs. 4B and 6A). The frequencies of all the bands in the high-frequency envelope, with the exception of the 855 cm^{-1} and 950 cm^{-1} bands, have shifted down. This shift indicates that Si(Al) coupling takes place in the two most polymerized structural units. In the analogous sodium-bearing melts, NS2NA2.5 and NS2CA2.5, only the three-dimensional network unit appeared to contain aluminum (Figs. 4B, 6A and 8B). The frequency of the antisymmetric stretch band for all bridging oxygens is at 1030 cm^{-1}, approximately the same as for NS2CA2.5, as would be expected because of the Al content of the melt is the same.

The addition of 7.5 mole % $CaAl_2O_4$ (CS2CA7.5) results in the spectrum shown in Fig. 8C (see also Table 5). With this concentration of Al_2O_3, the $^-$O–Si(Al)–O^0 symmetric stretch band has shifted to lower frequency so that the antisymmetric stretch band from the three-dimensional network unit (at 1145 cm^{-1}) may be discerned. The frequency of the composite antisymmetric stretch band corresponds with that in the analogous sodium system (Fig. 4D) as would be expected because the bulk Al contents of the two systems are similar (Table 1). The frequencies of the symmetric stretch bands from units with NBO/T = 2 and 1, respectively, have shifted more relative to their position in the Al-free system than they did analogous to the sodium system (Figs. 4 and 8).

The spectrum of quenched CS2CA15 melt (15 mole % Al_2O_3 added as $CaAl_2O_4$) shown in Figure 8D represents a continuing evolution of the trends from the less aluminous samples. No new structural interpretations are required. All the structural units in the melt have become more aluminous.

In the spectrum of CS2CA30 (30 mole % Al_2O_3 added as $CaAl_2O_4$), the high-frequency envelope has lost its structure in much the same way as in the system NS2CA30 (Figs. 6H and 8E). The bands within this envelope have been fitted in order to make the evolution of bands as a function of Al content internally consistent. In the low-frequency portion of the

spectrum, the 510 cm^{-1} band has increased in intensity so that it is now more intense than the 575 cm^{-1} band, reflecting the increased importance of three-dimensional network structures in this melt.

The spectrum of quenched CS2CA40 melt (40 mole % Al_2O_3 added as $CaAl_2O_4$) very closely mimics that of CS2CA30 (Figs. 8E and F), and no further comments are required.

The evolution of the frequencies of the stretch bands as a function of Al content in the system $CaSi_2O_5$–$CaAl_2O_4$ is shown in Figure 9. It can be seen from these data that the frequency of the 1050 cm^{-1} antisymmetric stretch band shifts at a rate similar to that in the previous two systems. This observation would be expected, as this band simply reflects the bulk Al content in all the structural units. The frequency shifts of the three symmetric stretch bands ($^-$O–Si(Al)–O$^-$, $^-$O–Si(Al)–O^0 and Si(Al)–O^0) indicate that the Al content of the three-dimensional network unit increases at a slower rate than in the systems NS2CA and NS2NA, whereas the Al contents of the sheet and chain units increase faster. That is, aluminum in a system where it is completely charge-balanced by Ca^{2+} is more evenly distributed between the individual structural units than when Na^+ is present.

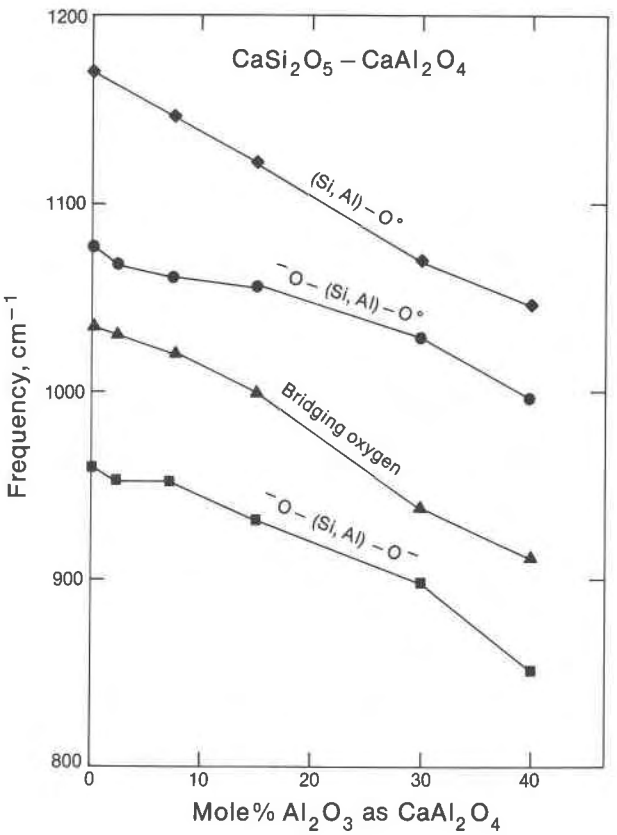

Fig. 9. Rate of change of important Raman bands in the system $CaSi_2O_5$–$CaAl_2O_4$ as a function of Al content (mole % on the basis of 5 oxygens).

Melts in the system CaO–SiO_2–Al_2O_3 with NBO/T greater than 1

A composition in the system CaO–SiO_2 was chosen to determine the influence of aluminum, added as Al_2O_3, on the melt structure. The composition, SW40 (Ca/Si = 0.67), is within the compositional range where equation 2 describes the coexisting structural units.

The spectra of SW40 + Al_2O_3 are shown in Figure 10, and detailed data are given in Table 6. The spectrum of aluminum-free quenched melt of SW40 composition has been discussed by Virgo *et al.* (1979) and Mysen *et al.* (1980d) and will be only briefly summarized here. The spectrum resembles that of $CaSi_2O_5$ in that it shows the bands indicative of symmetric Si–O^{2-} stretching at 855 cm^{-1}, symmetric $^-$O–Si–O$^-$ stretching at 960 cm^{-1}, symmetric $^-$O–Si–O^0 stretching at 1082 cm^{-1} and the cumulative antisymmetric stretch band at 1042 cm^{-1} (Fig. 10A). The weak band at 480 cm^{-1} in quenched $CaSi_2O_5$ melt (Fig. 8A) does not occur, nor is there one at 800 cm^{-1}. It is not likely, therefore, that there are any three-dimensional network units in this melt. As before, the 340 cm^{-1} band is tentatively assigned to oxygen vibrations in Ca–O polyhedra.

Addition of 5 wt.% Al_2O_3 to SW40 melt results in the spectrum in Figure 10B. Although no new bands have appeared, the original bands have shifted very significantly, and their relative intensities have changed. The 855 cm^{-1} band is very weak, and this result indicates that the proportion of monomers in this melt is greatly reduced relative to that in Al-free SW40 melt. The frequency of the 960 cm^{-1} band ($^-$O–Si–O$^-$ symmetric stretching) is shifted down to 933 cm^{-1}, and its intensity relative to the rest of the high-frequency envelope is greatly reduced. These observations indicate a significant amount of Al^{3+} in the chain unit, but a smaller proportion of such units in this melt relative to that in Al-free SW40 melt. The frequencies of the $^-$O–Si–O^0 symmetric stretch band and the Si–O^0 antisymmetric stretch bands have shifted by nearly 50 cm^{-1}, even more than the band at 933 cm^{-1}.

Addition of 7.5 wt.% Al_2O_3 results in a spectrum (Fig. 10C) that indicates a continuing evolution of

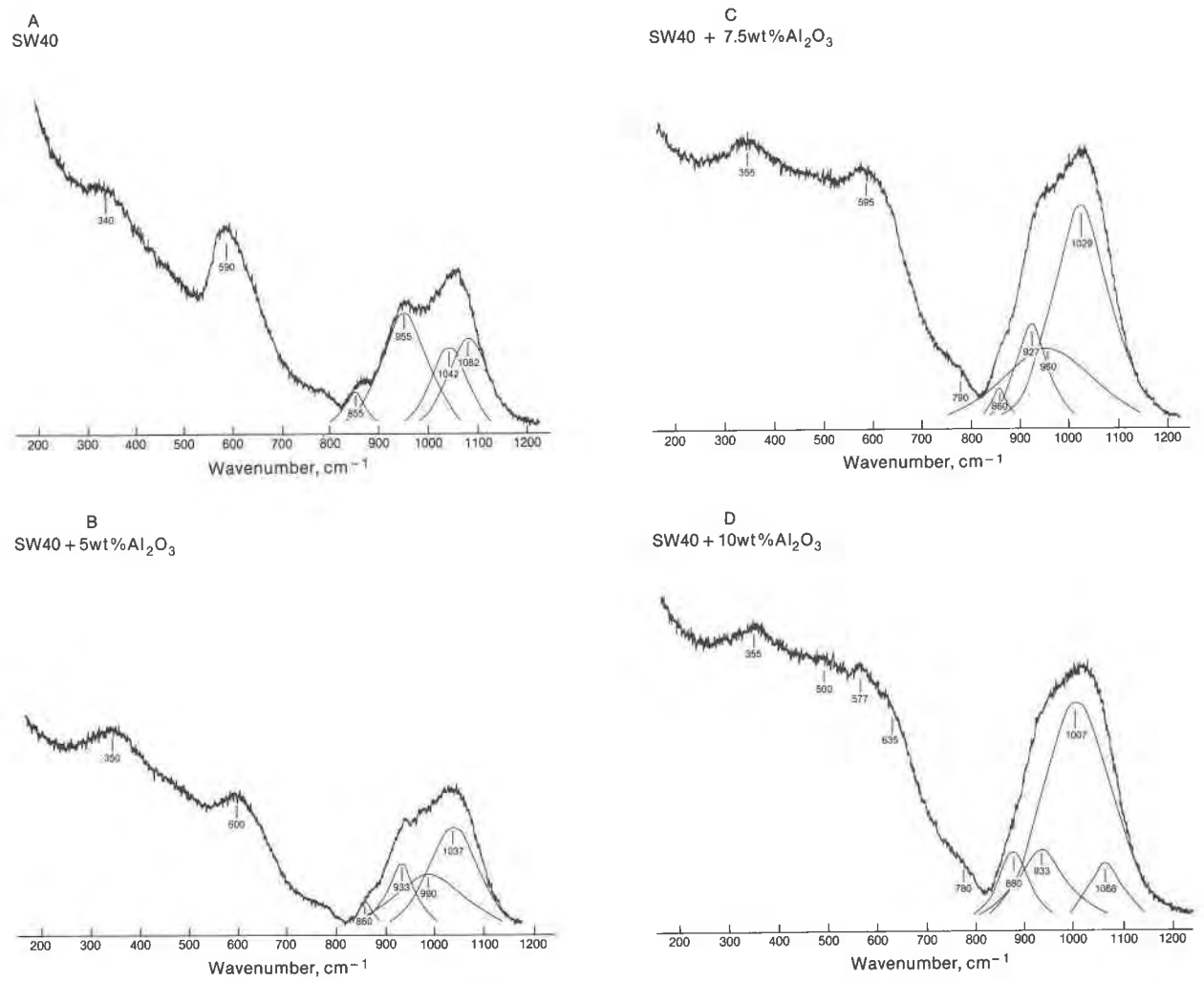

Fig. 10. Unpolarized Raman spectra of quenched melts on the join SW40–Al_2O_3 as a function of Al content (symbols as in Table 1).

the trends between the Al-free SW40 melt and that containing 5 wt.% Al_2O_3.

The Raman spectrum of SW40 + 10 wt.% Al_2O_3 is shown in Fig. 10D (see also Table 6). In this spectrum, several new bands have emerged compared with the spectrum of SW40 + 7.5 wt.% Al_2O_3. There is a weak, very broad band near 500 cm^{-1}, a shoulder near 800 cm^{-1} and another relatively weak band near 1068 cm^{-1}. These bands are interpreted to indicate the presence of aluminous, three-dimensional network units in this melt composition. There is no longer a band at 855 cm^{-1}. It is concluded, therefore, that monomers that occurred in the less aluminous SW40 melts are no longer there. The shoulder at 635 cm^{-1} most likely results from deformation in the structural unit with NBO/T = 2, as also indicated above for other compositions.

Table 6. Raman data on melts on the join SW40 + Al_2O_3

Comp.	Wavenumber, cm^{-1}									
SW40	340 w	–	590 ms,p	–	–	855 w,p	855 s,p	1042 m	1082 m,p	–
SW40 + 5 wt % Al_2O_3	350 mw	–	600 mw,p	–	–	860 vw,p	933 m,p	990 m	1037 ms,p	–
SW40 + 7.5 wt % Al_2O_3	355 w	–	595 w,p	–	790 vw	860 vw,p	927 m,p	960 m	1029 s,p	–
SW40 + 10 wt % Al_2O_3	355 vw	500 vw	577 w	635 (sh)	780 (sh)	–	880 mw,p	933 m	1007 s,p	1068 mw

Abbreviations as in Table 3.

Fig. 11 It can be seen from these data that in contrast to those for the systems $Na_2Si_2O_5$–$CaAl_2O_4$–$NaAlO_2$ and $CaSi_2O_5$–$CaAl_2O_4$

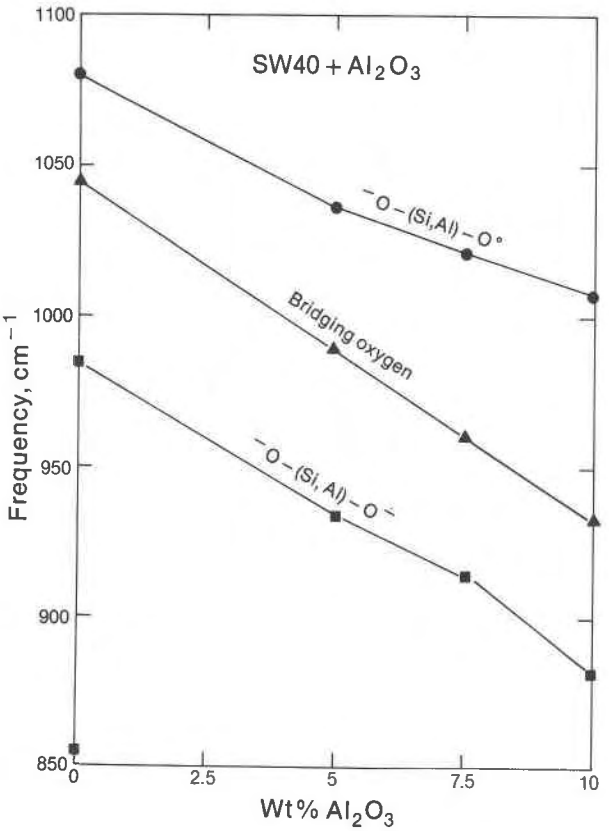

Fig. 11. Rate of change of important Raman bands in the system SW40–Al_2O_3 as a function of Al content.

(Figs. 5, 7 and 9), all the bands shift as a function of Al content in a nearly linear fashion. In the system SW40 + Al_2O_3, Al^{3+} is consequently distributed between all structural units at all times.

In summary, SW40 quenched melt evolves as do the quenched melts with aluminate added, that we discussed above. Importantly, Al_2O_3, when added to a melt that contains a network modifier in excess of that needed for local charge-balance of Al^{3+} in tetrahedral coordination, such as Ca^{2+}, remains in tetrahedral coordination.

Discussion

It is concluded that Al^{3+} is in tetrahedral coordination in silicate melts provided that charge-balancing cations like Na^+ or Ca^{2+} are available. It is likely, in view of the data of M. Taylor and Brown (1979b) on structures of melts of feldspar compositions, and the data of Riebling (1964) on melts in the system MgO–Al_2O_3–SiO_2, that other alkalies and alkaline earths will also charge-balance Al^{3+} in tetrahedral coordination.

The Raman spectroscopic data for melts on the join SAN6–SA10 (Fig. 3) indicate that nonbridging oxygens are formed when Na/Al is < 1. Nonbridging oxygens can be formed only by the destabilization of some of the tetrahedrally coordinated Al^{3+}. The principle of the release of Al^{3+} from tetrahedral coordination may be illustrated by the formalized equation:

$$Al(IV)Si_7O_{16}^- = Al^{3+}(VI) + 7SiO_2 + 2O^{2-}, \quad (4)$$

where $Al^{3+}(VI)$ denotes Al^{3+} as a network modifier (*e.g.*, VI-coordinated), SiO_2 is the silicate component with tetrahedrally coordinated Si^{4+}, and O^{2-} is the nonbridging oxygen formed as a result of the Al^{3+} in the aluminate leaving tetrahedral coordination. Equation 4 is written for the stoichiometry of composition SAN6. Analogous equations may be written for other aluminum–silicate ratios.

The Raman spectrum of SA10 indicates that all Al^{3+} is a network modifier in this melt composition. The NBO/Si for this composition may then be calculated (see Mysen *et al.*, 1980d, for calculation of NBO/Si and NBO/*T*), as shown in Table 1. According to Virgo *et al.* (1980) and Mysen *et al.* (1980d), a binary oxide–silica melt with NBO/Si = 0.394 (the value for SA10) has structural units that may be described by equation 3. This equation may be combined with equation 4 to describe the reaction along the join SAN6 as Na/Al is reduced below 1:

$$3Al(IV)Si_7O_{16}^- = 3Al^{3+}(VI) + 13SiO_2 + 2Si_2O_5^{2-} + 2Si_2O_6^{4-}, \quad (5)$$

As written, equation 5 rigorously describes the proportions in structural units in SA10 melt when the reaction has gone to completion. Anywhere along the join between SAN6 and SA10 there will be an equilibrium constant with a finite value, a value that will increase as Na/Al decreases. The formulae in equation 5 (SiO_2, $Si_2O_5^{2-}$ and $Si_2O_6^{4-}$) represent the structural units with average NBO/Si = 0, 1 and 2, respectively. In view of the fact that the frequencies of the ^-O–Si–O^- and ^-O–Si–O^0 symmetric stretch bands (NBO/Si = 2 and 1, respectively) remain in the position of Al-free chains and sheets for both SAN3 and SA10 composition, it is not likely that these structural units contain Al^{3+}. This conclusion is also supported by the data on the join $Na_2Si_2O_5$–$NaAlO_2$ (Fig. 4), which indicate that in Na^+-bearing systems with Al contents analogous to those of the melts on the SAN6–SA10 join, Al^{3+} in tetrahedral coordination will all be in three-dimensional network structures.

The addition of Al^{3+} to the melts with the proportion of metal cation equal to or exceeding that of Al^{3+}

always results in all Al^{3+} being in tetrahedral coordination. It appears, however, that the distribution of Al^{3+} between the structural units depends on the type of metal cation present and on the amount of Al^{3+} added to the systems. The extent to which Al^{3+} is distributed between the individual structural units may be monitored by the rate of decrease in frequency of the stretch bands in the high-frequency envelope as a function of Al content of the melt (Virgo *et al.*, 1979; Brawer and White, 1977; Mysen *et al.*, 1980d). The proportions of the individual structural units, however, will also vary with Al content as the NBO/*T* of the melts change as the proportion of tetrahedral cations increases with increasing Al content (Table 1). In both the CS2–CA and NS2–NA–CA systems, the NBO/*T* decreases below 1. It is likely, therefore, that the proportion of units with NBO/*T* = 2 and 1 will decrease, a suggestion also supported by the decrease in the intensity of the relevant Raman bands relative to those of three-dimensional network units. In the system SW40 + Al_2O_3 the Al-free melt has NBO/Si = 1.34 (Table 1). The value of this ratio passes through 1 near 7.5 wt.% Al_2O_3, a concentration that coincides with the appearance of Raman bands indicative of three-dimensional network units in the melt. It is concluded, therefore, that the proportion of sheet units increases and the proportion of chain and monomer units in the melt decreases in this concentration interval. Above 7.5 wt.% Al_2O_3 the proportion of all structural units with NBO/*T* greater than 0 will decrease and the proportion of three-dimensional network units will increase.

With the above qualifying comments in mind, the rate of change of stretch frequencies will be used to place bounds on the extent of Al^{3+} distribution between the structural units. The rate of change of the $^-$O–Si(Al)–O$^-$ (NBO/*T* = 2) and $^-$O–Si(Al)–O^0 (NBO/*T* = 1) symmetric stretch bands and the Si(Al)–O^0 (NBO/*T* = 0) antisymmetric stretch bands as a function of mole % Al_2O_3 added are shown in Table 7. The values of the frequencies have an uncertainty of about 5–10 cm^{-1}, however, which means that the uncertainties of these numbers are between 5 and 10% (relative).

In the system $Na_2Si_2O_5$–$NaAlO_2$ three compositional ranges within each of which Al^{3+} shows different distribution patterns between the structural units in the melt have been defined. Equation 3 may be modified to express the solution mechanisms of Al^{3+} in these compositional ranges.

In the system $Na_2Si_2O_5$–$NaAlO_2$ (NS2–NA), only the (Si,Al)–O^0 antisymmetric stretch band shifts within the first 10 mole % Al_2O_3. It is concluded, therefore, that all the added aluminum enters three-dimensional network structures.

Table 7. Rate of change of frequencies with Al_2O_3 (cm^{-1}/mole% Al_2O_3)

	0–10 mole %	10–20 mole %	20–40 mole %
	$Na_2Si_2O_5$–$NaAlO_2$		
(Si,Al)-O°	7.7	3.0	3.6
$^-$O-(Si,Al)-O°	0	1.5	1.7
$^-$O-(Si,Al)-O$^-$	0	0	1.2
	$Na_2Si_2O_5$–$CaAl_2O_4$		
(Si,Al)-O°	n.d.	5.3	5.3
$^-$O-(Si,Al)-O°	-	2.5	3.1
$^-$O-(Si,Al)-O$^-$	-	-	1.3
	$CaSi_2O_5$–$CaAl_2O_4$		
	0–10 mole %	10–40 mole %	
(Si,Al)-O°	3.3	3.3	
$^-$O-(Si,Al)-O°	2.7	2.4	
$^-$O-(Si,Al)-O$^-$	-	1.3	
	SW40 + Al_2O_3		
	0–12.60 mole %	12.69–16.61 mole %	
$^-$O-(Si,Al)-O°	4.2	5.6	
$^-$O-(Si,Al)-O$^-$	2.2	12.0	

Notations: (Si,Al)-O°: (Si,Al) coupled antisymmetric vibrations in three-dimensional network structures (NBO/T = 0). $^-$O-(Si,Al)-O°: (Si,Al) coupled symmetric stretch vibrations in structural units with NBO/T = 1. $^-$O-(Si,Al)-O$^-$: (Si,Al) coupled symmetric stretch vibrations in structural units with NBO/T = 2.
n.d., not determined.
*Al_2O_3 is added as $CaAl_2O_4$ and $NaAlO_2$. The mole % Al_2O_3 is calculated from the bulk compositions after addition of aluminate.

Let the aluminate structural units with NBO/Al = 0, 1 and 2 be denoted $NaAlO_2$, $(NaAl)_2O_5^{2-}$ and $(NaAl)_2O_6^{4-}$, respectively. In the range 10–20 mole % Al_2O_3, the equilibrium is

$$2NaAlO_2 + 3Si_2O_5^{2-} = 4SiO_2 + Si_2O_6^{4-} + (NaAl)_2O_5^{2-}. \quad (6)$$

In the concentration range 20–40 mole % Al_2O_3 the equilibrium is

$$4NaAlO_2 + 5Si_2O_5^{2-} = 8SiO_2 + Si_2O_6^{4-} + (NaAl)_2O_5^{2-} + (NaAl)_2O_6^{4-}. \quad (7)$$

In both equations 6 and 7 aluminate and silicate components with identical NBO/*T* are randomly mixed.

The data summarized in Table 7 for the system $CaSi_2O_5$–$CaAl_2O_4$ may be treated similarly to those for the system $Na_2Si_2O_5$–$NaAlO_2$ above. It is noted that in the calcium system, only two compositional

regions may be discerned. In the range up to 10 mole % Al_2O_3 added as $CaAl_2O_4$, aluminum enters both the three-dimensional network units and the sheet units because both the (Si,Al)–O^0 antisymmetric stretch band and the $^-$O–Si(Al)–O^0 symmetric stretch band shift down as aluminum is dissolved. In this concentration range equation 3 may be changed to accommodate the formation of $CaAl_2O_5^{2-}$ and $CaAl_2O_4$ structural units, both of which mix randomly with the silicate counterparts:

$$CaAl_2O_4 + 3Si_2O_5^{2-} = 4SiO_2 + Si_2O_6^{4-} + CaAl_2O_5^{2-}. \quad (8)$$

Equation 8 is identical to equation (6) except that Na^+ has been exchanged with Ca^{2+}.

In the remainder of the compositional range in the system CS2–CA, aluminum enters all structural units in which it mixes randomly with the silicate counterparts:

$$2CaAl_2O_4 + 5Si_2O_5^{2-} = 8SiO_2 + Si_2O_6^{4-} + CaAl_2O_5^{2-} + CaAl_2O_6^{4-}, \quad (9)$$

an equation that is similar to equation 8 above.

It appears that with Ca^{2+} as the charge-balancing cation, aluminum is more evenly distributed between the structural units than when Na^+ is the charge-balancing cation. This conclusion may imply that sodium-stabilized aluminate is more stable than calcium-stabilized aluminate complexes, a suggestion also made by Bottinga and Weill (1972). This conclusion may also aid in deciding whether Na^+ in NS2–CA melts remains a network modifier or exchanges with the added Ca^{2+} in $CaAl_2O_4$ to form $(NaAl)^{4+}$ complexes with Ca^{2+} as the network-modifying cation. From the data in Table 7 it can be seen that the evolution of Al distribution between structural units as a function of aluminum content is similar to that in the system NS2–NA but differs from that in the system CS2–CA. It is suggested, therefore, that the Na^+ and Ca^{2+} are, in fact, exchanged.

In the system SW40 + Al_2O_3 no additional metal cation was added with aluminum. The aluminate complexes thus formed will therefore derive their charge-balance from the network-modifying Ca^{2+} already present. The reaction may, in principle, be expressed by combining equation 2 (NBO/Si of SW40 is 1.34) with the formation of aluminate chains and sheets:

$$2Al_2O_3 + 2Ca^{2+} + 8Si_2O_6^{4-} = 7Si_2O_5^{2-} + 2SiO_4^{4-} + CaAl_2O_5^{2-} + CaAl_2O_6^{4-}. \quad (10)$$

As can be seen from the calculated relative changes of NBO/T as a function of mole % Al_2O_3 added to these systems (Table 8), this process is a more effective means of polymerizing the melt than adding charge-balanced aluminum as in the systems NS2–NA, NS2–CA and CS2–CA.

The rates of change of the frequencies of the stretch vibrations may also be used to estimate minimum values of partition coefficients of Al^{3+} between the structural units. Such values may be derived by simply dividing the rates with each other over compositional ranges where the rates are rather linear. As can be seen from the data in Figures 4–11, this assumption is not entirely correct but is used here as a means of estimating the values. Even though Al^{3+} and Si^{4+} appear to mix randomly in each structural unit, the proportion of the units changes; thus the nonlinearity in Figures 5, 7 and 9 results. For all the systems involving three-dimensional network units, the values, expressed as "3D-sheet" and "3D-chain," will be minimum values because the proportions of chains and sheets decrease and the proportion of 3D increases. Even so, it appears from the results of such calculations (Table 9) that in all systems Al^{3+} shows a preference for 3D over sheet and for sheet over chain. The preference is less pronounced when Ca^{2+} is a charge-balancing cation than when Na^+ is.

Table 8. Relative change of NBO/T per mole % Al_2O_3

NBO/T of Al^{3+} units present	Rate of change (%)
$Na_2Si_2O_5$–$NaAlO_2$	
0	1.34
0, 1	1.875
0, 1, 2	1.00
$Na_2Si_2O_5$–$CaAl_2O_4$	
0	1.34
1, 2	1.875
0, 1, 2	1.00
$CaSi_2O_5$–$CaAl_2O_4$	
0	1.34
0, 1	1.875
0, 1, 2	1.00
CaO–SiO_2–Al_2O_3	
0	2.00
0, 1	2.00
0, 1, 2	2.00

Table 9. Estimated aluminum partition coefficients

	0-10 mole %	10-20 mole %	20-40 mole %
	$Na_2Si_2O_5$-$NaAlO_2$		
Al^{3D}/Al^{sheet}	1	2.0	2.1
Al^{3D}/Al^{chain}	1	1	3.0
Al^{sheet}/Al^{chain}	-	1	1.4
	$Na_2Si_2O_5$-$CaAl_2O_4$		
Al^{3D}/Al^{sheet}	-	2.1	2.5
Al^{3D}/Al^{chain}	-	1	4.2
Al^{sheet}/Al^{chain}	-	1	2.5
	$CaSi_2O_5$-$CaAl_2O_4$		
	0-10 mole %	10-40 mole %	
Al^{3D}/Al^{sheet}	1.2	1.4	
Al^{3D}/Al^{chain}	1	2.5	
Al^{sheet}/Al^{chain}	1	1.8	

Notations: 3D: rate of change of (Si,Al)-O° antisymmetric stretch vibration. Sheet: rate of change of $^-$O-(Si,Al)-O° symmetric stretch vibration. Chain: rate of change of $^-$O-(Si,Al)-O$^-$ symmetric stretch vibration.

Implications for properties of natural magma

On the basis of the results presented here and those already available (Virgo *et al.,* 1979, 1980; Mysen *et al.,* 1980a,b,c), it is possible to calculate the proportions of anionic structural units in silicate melts from their bulk chemical analyses. Mysen *et al.* (1980a,b) concluded that P^{5+} and Ti^{4+} are in tetrahedral coordination in silicate melts. These cations are found in separate units, however, rather than mixed with Si^{4+} or Al^{3+}. Phosphorus generally occurs in chain units, whereas Ti^{4+} occupies the same type of structural units as Si^{4+}, although Ti^{4+} does not mix with Si^{4+}. Ferric iron is also found in separate units rather than in random mixtures with Si^{4+}. Furthermore, Mysen *et al.* (1980c) found that Fe^{3+} is in tetrahedral coordination only when charge-balanced with alkali metals. The latter conclusion implies that ferric iron is a network former only in the rather uncommon peralkaline igneous melts.

On the basis of the above considerations and the data presented in this report, it is possible to calculate the distribution of tetrahedrally coordinated cations in igneous melts from their bulk chemical composition. The ratio of nonbridging oxygens per tetrahedral cation may also be computed. In order to carry out this calculation, it is necessary to recast analyses to atomic proportions. After this has been done, Fe^{3+} is assigned to tetrahedral coordination only if alkali metals are present after Al^{3+} is balanced (Bottinga and Weill, 1972). Titanium and phosphorus are always in tetrahedral coordination. The phosphate complex either is an aluminate complex or is stabilized with alkali metals or alkaline earths.

The calculations are carried out as follows. The tetrahedrally coordinated cations (*T*-cations) are calculated first. Due to local charge-balance constraints (see also Wood and Hess, 1980), all tetrahedrally coordinated cations have an effective charge of 4+. For cations which differ from 4+ [*e.g.,* Fe^{3+}, Al^{3+}, P^{5+}), this balance is accomplished by balancing with monovalent (alkali metals) or divalent cations (*e.g.,* alkaline earths). The present and other data (see, for example, Wood and Hess, 1980; and Bottinga and Weill, 1972) indicate that alkali-balanced aluminate complexes are more stable than those balanced by alkaline earths. Consequently, after a chemical analysis is recast to atomic proportions, alkali aluminate complexes [$(NaAl)^{4+}$ and (KAl^{4+})] are computed first. Only if a melt is peralkaline [(Na+K) > Al], will Fe^{3+} be in tetrahedral coordination. The amount of tetrahedral Fe^{3+} is given by the relation:

$$Fe^{3+}(IV) = (Na^+ + K^+) - Al^{3+} \qquad (11)$$

If $Al^{3+} > (Na^+ + K^+)$ (as is commonly the case), Fe^{3+} is a network modifier. Any excess Al^{3+} over that which can be balanced with alkalies will be balanced with alkaline earths. If there is an excess Al^{3+} over $(Na^+ + K^+ + Ca^{2+} + Mg^{2+})$, this Al^{3+} is a network modifier. In most natural magmas (> 99% according to compilation by Chayes, 1975), $Al^{3+} < (Na + K^+ + Ca^{2+} + Mg^{2+})$. Consequently, aluminum generally is a network-former in natural magma. Only the excess $(Ca^{2+} + Mg^{2+})$ after balancing Al^{3+} is network-modifying. The NBO/*T* is calculated by adding up all tetrahedrally coordinated cations, multiplying by four and subtracting this number from the proportion of oxygen multiplied by two. This difference is the total number of nonbridging oxygens in the melt. The resulting number is divided by the number of tetrahedral cations in the structure. This procedure is used in both Tables 1 and 10. It can be seen from the data in Table 10 that basalts have NBO/*T* between 0.9 and 0.6. On the basis of these data, it is concluded that such rocks consist of structural units that have chain, sheet and three-dimensional network units in their structure. Andesitic melts cluster at about 0.3, whereas more acidic rocks have an even smaller NBO/*T*. Few igneous rocks have NBO/*T* greater than 1. Those that do include basanites, certain nephelinites, picrites and komatiites.

Table 10. Percent distribution of tetrahedral cations in igneous melts

	1	2	3	4	5	6	7	8	9	10
NBO/T	0.075	0.129	0.335	0.649	0.929	1.008	0.864	0.754	0.060	0.435
$(Si^{4+})^0$	40.7	38.3	36.7	35.5	35.1	35.8	34.9	41.2	36.6	37.2
$(Si^{4+})^1$	20.4	19.1	18.4	17.7	17.5	17.9	17.4	20.6	18.3	18.6
$(Si^{4+})^2$	20.4	19.1	18.4	17.7	17.5	17.9	17.4	20.6	18.3	18.6
$(Al^{3+})^0$	10.2	13.2	15.0	15.9	15.5	15.7	15.6	8.8	15.4	14.5
$(Al^{3+})^1$	4.6	5.8	6.5	6.7	6.7	6.6	6.8	4.2	6.5	6.1
$(Al^{3+})^2$	3.2	3.8	4.1	4.6	4.3	4.1	4.4	2.9	4.1	3.9
Ti^{4+}	0.3	0.5	0.8	1.7	2.9	2.0	3.2	0.2	0.7	1.1
P^{5+}	0.1	0.2	0.2	0.2	0.5	-	0.3	-	0.1	0.1
Fe^{3+}	-	-	-	-	-	-	-	1.5	-	-
$(Si/(Si+Al))^0$	0.80	0.74	0.71	0.69	0.69	0.70	0.69	0.82	0.70	0.72
$(Si/(Si+Al))^1$	0.81	0.77	0.74	0.73	0.72	0.73	0.72	0.83	0.74	0.75
$(Si/(Si+Al))^2$	0.86	0.83	0.82	0.79	0.80	0.81	0.80	0.88	0.82	0.83
$(Si/(Si+Al)^r$	0.82	0.77	0.74	0.73	0.73	0.73	0.72	0.84	0.74	0.73

Rocks 1-5 (Chayes, 1975): 1, rhyolite; 2, dacite; 3, andesite; 4, subalkaline basalt; 5, alkaline basalt. Rocks 6-8 (Scarfe and Hamilton, 1980): 6, alkali basalt (PAP); 7, hawaiite (8125-50/6397); 8, commendite (8/25-54/6345). Rocks 9 and 10 (Scarfe, 1977): 9, basaltic andesite (Mt. Pihanga, New Zealand); 10, tholeiite (Antrim, N. Ireland).

Notations 0, 1 and 2 refer to structural units with NBO/T = 0, 1 and 2, respectively; r refers to bulk rock.

The aluminum distribution between structural units may be evaluated from the above aluminum distribution data. Alkali aluminates are calculated first, then alkaline earth aluminates. The distribution of silicon is based on equation 3. On this basis, the distribution of tetrahedral cations between structural units in natural magma may be calculated (Table 10). The Si/(Si+Al) of the individual units may also be derived (Table 9). As would be expected, the value of the bulk Si/(Si+Al) of the rock falls within the range of Si/(Si+Al) of the individual units.

In all the rock analyses considered, the three-dimensional network units are the most aluminous, then the sheet and chain units. This conclusion is expected in view of the fact that Al^{3+} always shows a preference for the most polymerized structural unit in the melt. It is also noted that generally the more acidic rocks show the greatest values of Si/(Si+Al) (Table 10). In fact Si/(Si+Al) of the structural units is positively correlated with Mg/(Mg+Fe^{2+}) of the rock (Fig. 12).

The ratio of NBO/T is positively correlated with the activation energy of viscous flow ($E\eta$) of the melt (Fig. 13). The correlation would be expected in view of the positive correlation between activation energy and NBO/Si on simple binary metal oxide–silicate joins (Bockris and Reddy, 1970; Mysen *et al.*, 1980d). It is noted, however, that there is considerable scatter, an observation that may be understood in view of the aluminous nature of the structural units involved. The activation energy of viscous flow decreases with decreasing Si/(Si+Al) of the system (Riebling, 1966) as the strength of bonds that are broken during viscous flow decreases the lower the Si/(Si+Al) (T. D. Taylor and Rindone, 1970). It can be seen from the

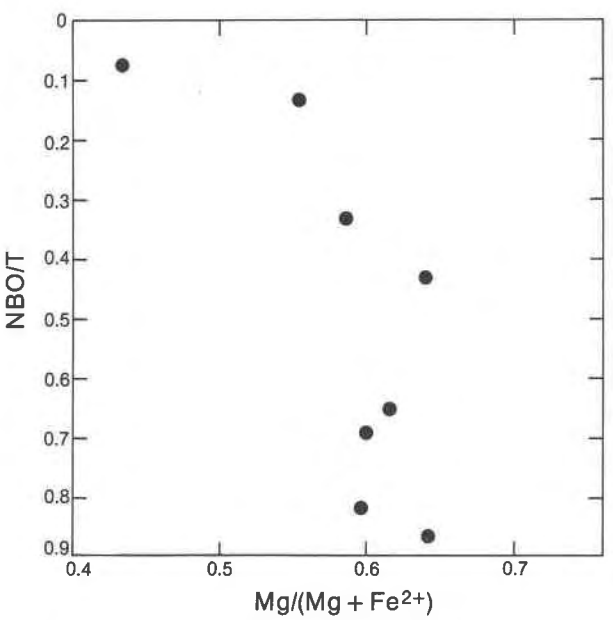

Fig. 12. NBO/T of igneous melts as a function of their Mg/(Mg+Fe^{2+}) (symbols as in Table 10).

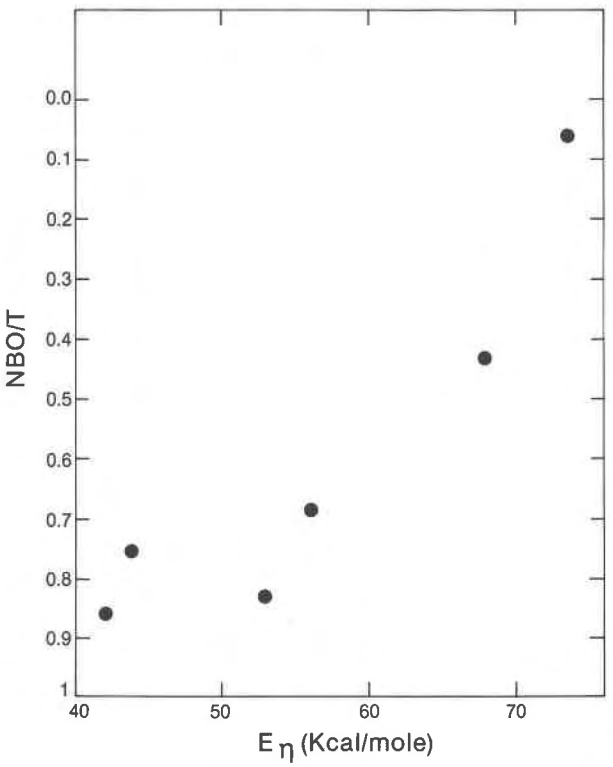

Fig. 13. NBO/T of igneous melts *vs.* activation energy of their viscous flow at 1 atm pressure (viscosity data from Scarfe, 1977, and Scarfe and Hamilton, 1980).

data in Figure 13 that the most aluminous melts show the greatest deviation from linearity between $E\eta$ and NBO/T.

Acknowledgments

Critical reviews by Drs. T. M. Benjamin, F. Seifert, and H. S. Yoder, Jr., are appreciated. This research was supported partially by National Science Foundation grant EAR 7911313 and partially by the Carnegie Institution of Washington.

References

Bates, J. B., Hendricks, R. W., and Shaffer, L. B. (1974) Neutron irradiation effects and the structure of non-crystalline SiO_2. Journal of Chemical Physics, 61, 4163–4176.

Bell, R. J. and Dean, P. (1972) Localization of phonons in vitreous silica and related glasses. In R. W. Douglas and B. Ellis, Eds., International Conference on the Physics of Non-Crystalline Solids, 3d, University of Sheffield, 1970, p. 443–452. Wiley-Interscience, London.

Bockris, J. O'M. and Reddy, A. K. N. (1970) Modern Electrochemistry, Vol. 1. Plenum Press, New York.

Bottinga, Y. and Weill, D. F. (1972) The viscosity of magmatic silicate liquids: A model for calculation. American Journal of Science, 272, 438–475.

Brawer, S. A. (1975) Theory of the vibrational spectra of some network and molecular glasses. Physical Review, B, 11, 3173–3194.

Brawer, S. A. and White, W. B. (1975) Raman spectroscopic investigation of the structure of silicate glasses. I. The binary silicate glasses. Journal of Chemical Physics, 63, 2421–2432.

Brawer, S. A. and White, W. B. (1977) Raman spectroscopic investigation of the structure of silicate glasses. II. Soda-alkaline earth-alumina ternary and quarternary glasses. Journal of Non-Crystalline Solids, 23, 261–278.

Chayes, F. (1975) Average compositions of the commoner Cenozoic igneous rocks. Carnegie Institution of Washington Year Book 74, 547–549.

Cukiermann, M. and Uhlmann, D. R. (1973) Viscosity of liquid anorthotite. Journal of Geophysical Research, 78, 4920–4924.

Day, D. E. and Rindone, G. E. (1962a) Properties of soda aluminosilicate glasses: II. Internal friction. Journal of the American Ceramic Society, 45, 496–504.

Day, D. E. and Rindone, G. E. (1962b) Properties of soda aluminosilicate glasses: III. Coordination of aluminum ions. Journal of the American Ceramic Society, 45, 579–580.

Etchepare, J. (1972) Study by Raman spectroscopy of crystalline and glassy diopside. In R. W Douglas and B. Ellis, Eds., Amorphous Materials, p. 337–346. Wiley-Interscience, New York.

Furukawa, T. and White, W. B. (1980) Raman spectroscopic investigation of the structure of silicate glasses. III. Alkali-silicogermanates. Journal of Chemical Physics, in press.

Galeener, F. L. and Lucovsky, G. (1976) Longitudinal optical vibrations in glasses: SiO_2 and GeO_2. Physical Review Letters, 37, 1474–1478.

Galeener, F. L. and Mikkelsen, J. C. (1979) The Raman spectra of the structure of pure vitreous P_2O_5. Solid State Communications, 20, 505–510.

Gaskell, P. M. (1975) Construction of a model for amorphous tetrahedral materials using ordered units. Philosophical Magazine, 32, 211–229.

Gaskell, P. M. and Mistry, A. B. (1975) High-resolution electron microscopy of small amorphous silica particles. Philosophical Magazine, 32, 245–251.

Kushiro, I. (1975) On the nature of silicate melt and its significance in magma genesis: Regularities in the shift of liquidus boundaries involving olivine, pyroxene, and silica minerals. American Journal of Science, 275, 411–431.

Kushiro, I. (1976) Changes in viscosity and structure of melt of $NaAlSi_2O_6$ composition at high pressures. Journal of Geophysical Research, 81, 6347–6350.

Kushiro, I. (1978) Viscosity and structural changes of albite ($NaAlSi_2O_8$) melt at high pressure. Earth and Planetary Science Letters, 41, 87–91.

Lacey, E. D. (1963) Aluminum in glasses and melts. Physics and Chemistry of Glasses, 4, 234–238.

Lacey, E. D. (1968) Structure transition in alkali silicate glasses. Journal of the American Ceramic Society, 51, 150–157.

Lazarev, A. N. (1972) Vibrational Spectra and Structure of Silicates. Consultants Bureau, New York.

Lucovsky, G. (1979a) Spectroscopic evidence for valence-alternation pair defects in vitrous SiO_2. Philosophical Magazine, 39, 513–531.

Lucovsky, G. (1979b) Defect-controlled carrier transport in amorphous silica. Philosophical Magazine, 39, 531–541.

Mysen, B. O. (1976) The role of volatiles in silicate melts: Solubility of carbon dioxide and water in feldspar, pyroxene and feldspathoid melts to 30 kb and 1625°C. American Journal of Science, 276, 969–996.

Mysen, B. O. and Virgo, D. (1978) Influence of pressure, temperature and bulk composition on melt structures in the system $NaAlSi_2O_6$–$NaFe^{3+}Si_2O_6$. American Journal of Science, 278, 1307–1322.

Mysen, B. O., Ryerson, F. J., and Virgo, D. (1980a) The influence of TiO_2 on the structure and derivative properties of silicate melts. American Mineralogist, 65, 1150–1165.

Mysen, B. O., Ryerson, F. J., and Virgo, D. (1980b) The structural role of phosphorus in silicate melts. American Mineralogist, 66, 106–117.

Mysen, B. O., Seifert, F., and Virgo, D. (1980c) Structure and redox equilibria of iron-bearing silicate melts. American Mineralogist, 65, 867–884.

Mysen, B. O., Virgo, D., and Scarfe, C. M. (1980d) Relations between the anionic structure and viscosity of silicate melts: A Raman spectroscopic study at 1 atmosphere and at high pressure. American Mineralogist, 65, 690–711.

Riebling, E. F. (1964) Structure of magnesium silicate liquids at 1700°C. Canadian Journal of Chemistry, 42, 2811–2821.

Riebling, E. F. (1966) Structure of sodium aluminosilicate melts containing at least 50 mole % SiO_2 at 1500°C. Journal of Chemical Physics, 44, 2857–2865.

Riebling, E. F. (1968) Structural similarities between a glass and its melt. Journal of the American Ceramic Society, 51, 143–149.

Scarfe, C. M. (1977) Viscosity of some basaltic glasses at one atmosphere. Canadian Mineralogist, 15, 190–194.

Scarfe, C. M., and Hamilton, T. S. (1980) Viscosity of lavas from the Level Mountain volcanic center, northern British Columbia, Carnegie Institution of Washington Year Book 79, in press.

Sharma, S. K., Virgo, D., and Mysen, B. O. (1978) Structure of glasses and melts of $Na_2O \bullet xSiO_2$ (x = 1, 2, 3) composition from Raman spectroscopy. Carnegie Institution of Washington Year Book, 77, 649–652.

Sweet, J. R. and White, W. B. (1969) Study of sodium silicate glasses and liquids by infrared spectroscopy. Physics and Chemistry of Glasses, 10, 246–251.

Taylor, M. and Brown, G. E. (1979a) Structure of mineral glasses. I. The feldspar glasses, $NaAlSi_3O_8$, $KAlSi_3O_8$, $CaAl_2Si_2O_8$. Geochimica et Cosmochimica Acta, 43, 61–77.

Taylor, M. and Brown, G. E. (1969b) Structure of mineral glasses. II. The SiO_2–$NaAlSiO_4$ join. Geochimica et Cosmochimica Acta, 43, 1467–1475.

Taylor, M., Brown, G. E., and Fenn, P. M. (1980) Structure of silicate mineral glasses. III. $NaAlSi_3O_8$ supercooled liquid at 805°C and the effects of thermal history. Geochimica et Cosmochimica Acta, 44, 109–119.

Taylor, T. D. and Rindone, G. E. (1970) Properties of soda aluminosilicate glasses: V. Low-temperature viscosities. Journal of the American Ceramic Society, 53, 692–695.

Verweij, H. (1979a) Raman study of the structure of alkali germanosilicate glasses. I. Sodium and potassium metagermanosilicate glasses. Journal of Non-Crystalline Solids, 33, 41–53.

Verweij, H. (1979b) Raman study of the structure of alkali germanosilicate glasses. II. Lithium, sodium and potassium digermanosilicate glasses. Journal of Non-Crystalline Solids, 33, 55–69.

Virgo, D., Mysen, B. O., and Kushiro, I. (1980) Anionic constitution of silicate melts quenched at 1 atm from Raman spectroscopy: Implications for the structure of igneous melts. Science, 208, 1371–1373.

Virgo, D., Mysen, B. O., and Seifert, F. (1979) Quenched melt structures in the system $NaAlSiO_4$–$CaMgSi_2O_6$–Mg_2SiO_4–SiO_2 at 1 atm. Carnegie Institution of Washington Year Book, 78, 506–511.

Waff, H. S. (1975) Pressure-induced coordination changes in magmatic liquids. Geophysical Research Letters, 2, 193–196.

Wood, M. I. and Hess, P. C. (1980) The structural role of Al_2O_3 and TiO_2 in immiscible silicate liquids in the system SiO_2–MgO–CaO–FeO–TiO_2–Al_2O_3. Contributions to Mineralogy and Petrology, 72, 319–328.

Manuscript received, October 10, 1980;
accepted for publication, March 9, 1981.